



## **EU Cloud Intercomparison, Process Study & Evaluation Project**

**Grant agreement no. 244067**

Deliverable D2.8 "Interpretation of the spread of cloud and precipitation responses among models, in interaction with WP3 and WP4"

Part I: Interpretation of the spread of cloud responses among models.

Delivery date: Month48 (Jan 2014)

January 2014



## Part I: Interpretation of the spread of cloud responses among models.

Mark Webb, Sandrine Bony, Stephan de Roode, Bjorn Stevens and Pier Siebesma.

### 1. Introduction

Cloud Feedbacks in Earth System Models (ESMs) remain the largest source of uncertainty in projections of future climate. Consequently, one of the central aims of EUCLIPSE has been to develop our physical understanding of how cloud processes respond to and feed back on climate change, and of the reasons for inter-model differences in these cloud feedbacks.

WP2, entitled “Climate Model Evaluation and Analysis” has been (amongst other things) responsible for quantifying and interpreting the inter-model spread of climate sensitivity and cloud feedback from the models. This includes identifying the regions, the cloud regimes and the meteorological conditions primarily responsible for this spread, and exploring the mechanisms that control the different model responses. WP3, entitled “Process Level Evaluation” aims to understand the processes responsible for the responses of boundary layer clouds in idealised and future climate conditions through the use of LES (Large Eddy Simulation) models, idealised simple models such as boundary layer mixed layer models (MLMs) and Single Column Model (SCM) versions of the GCMs. WP4, entitled “Sensitivity experiments and hypothesis testing” has been responsible for developing physical hypotheses relating to cloud feedback mechanisms, and testing them by performing sensitivity experiments with the GCMs. This report summarises progress on the interpretation of the spread of cloud responses among models, drawing on developments within all three of these work packages.

This report is structured as follows. In Section 2 we review results from WP2 quantifying the forcings, feedbacks and climate sensitivity in the CMIP5 models, and summarise work from WP2 and WP3 identifying the regions, the cloud regimes and the meteorological conditions primarily responsible for this spread in the GCMs. In Section 3 we review the work on process based understanding using SCMs and LES models from WP3, and use it to interpret the GCM results. Section 4 reviews GCM sensitivity experiments performed in WP4 and the implications for interpreting inter-model spread in cloud feedback. We present our concluding remarks in Section 5.

### 2. Identification of the regions, cloud regimes and meteorological conditions responsible for the spread in cloud responses and climate sensitivity.

#### 2.1 *Global forcings, feedbacks and climate sensitivity in the CMIP5 models*

Equilibrium climate sensitivity (ECS) is defined as the global equilibrium surface-air-temperature change in response to instantaneous doubling of atmospheric CO<sub>2</sub> concentration. Although this is clearly not a realistic scenario, ECS is a convenient way of quantifying the joint effect of forcing and feedback, which are separately quantities of practical interest for understanding and predicting transient climate change. Recently, a new generation of climate models, participating in CMIP5, has been developed. Diagnosing the forcings, feedbacks and ECS in each of these models is a first step to identifying and understanding sources of uncertainty in their climate projections.

CO<sub>2</sub> forcings and feedbacks have been quantified across the available CMIP5 coupled atmosphere-ocean general circulation models (AOGCMs) using multiple methodologies. First, simulations forced by an abrupt quadrupling of atmospheric carbon dioxide concentration were analysed applying the linear forcing-feedback regression analysis of Gregory et al. (2004) to the ensemble of AOGCMs (Andrews et al. 2012). The range of equilibrium climate sensitivity was found to be 2.1-4.7K, similar to that derived from CMIP3 models (2.1-4.4K), and differences in cloud feedbacks continue to make the largest contribution to this range. Additionally, the radiative kernel approach of Soden and Held (2006) was used to assess the contributions of climate feedbacks and adjustments associated with water vapour, temperature lapse rate, clouds and surface albedo in the spread of climate sensitivity (Vial et al. 2013). This analysis confirmed again the dominant role of cloud feedbacks in inter-model spread in climate sensitivity. Fast tropospheric cloud adjustments to CO<sub>2</sub> (Gregory and Webb, 2008) were also found contribute to the spread, but these (and CO<sub>2</sub> forcing generally) contribute to a much lesser extent than cloud feedbacks (Andrews et al. 2012, Vial et al. 2013). More details of this work are available in Deliverable Report D2.6.

## *2.2 Contributions from different regions and regimes*

The regions, cloud regimes and meteorological conditions responsible for the spread in cloud responses in the models have been examined in a number of ways in WP2. Vial et al. (2013) not only quantified the contributions of cloud adjustments and feedbacks to inter-model spread in climate sensitivity in the AOGCMs, but also assessed the contributions to the spread from different regions and from within dynamical regimes over the tropical oceans. Figure 1 shows that the tropical regions between 30N/S explain more than half of the inter-model spread in all quantities shown, except surface albedo which is dominated by sea ice and snow feedbacks at higher latitudes. The inter-model differences in tropical cloud feedbacks contribute more than twice as much as the higher latitude regions combined.

Vial et al. (2013) also composited the coupled model cloud feedbacks in the tropics into regimes of 500mb pressure velocity, and separated these into contributions from a ‘thermodynamic’ component representing changes within each circulation regime, and a ‘dynamic’ component which represents changes due to shifts in the populations of the different regimes. As was the case in the CMIP3 models (Bony and Dufresne, 2005), the thermodynamic term makes a larger contribution to the differences in feedbacks between low and high sensitivity models. Thermodynamic components show largest differences between low and high sensitivity models in regions of weak-moderate subsidence, where shallow clouds such as stratocumulus and trade cumulus predominate (Figure 2). These are mainly due to the shortwave component, as found previously.

As part of the second phase of the Cloud Feedback Model Intercomparison Project (CFMIP-2), new cloud feedback experiments were added to the CMIP5 experimental design (Taylor et al. 2011), which included additional process diagnostics designed to support investigation of the physical mechanisms underlying cloud feedbacks and adjustments (Bony et al. 2011). These comprise AMIP experiments forced with 30 years of observed SSTs, and +4K global mean SST perturbation experiments, one where AMIP SSTs are increased uniformly by 4K (amip4K) and another where a patterned SST perturbation with a global mean of +4K is applied, based on a composite SST response from coupled models in CMIP3

(amipFuture). Also included were CO<sub>2</sub> quadrupling experiments with SSTs specified as in the AMIP experiments (amip4xCO<sub>2</sub>), to support the analysis of cloud adjustments which occur in response to CO<sub>2</sub> quadrupling but in the absence of SST changes. These CFMIP atmosphere-only experiments were included for a number of reasons. First, they support a cleaner separation between forcings and feedbacks than is possible in coupled models. Second, because they are relatively short, and computationally inexpensive compared to coupled model experiments, a more comprehensive set of process diagnostics can be included. Finally, their relative computational efficiency and lack of an interactive ocean makes them well suited for sensitivity experiments which can be used to test physical hypotheses relating to cloud feedback mechanisms.

Deliverable D2.7 summarised work within WP2 to assess the contribution of difference cloud regimes to inter-model spread in cloud feedbacks and adjustments in these experiments. Figure 3 shows the relative contributions of different geographical regions to inter-model spread in cloud feedbacks and cloud adjustments in the CMIP3/CFMIP-1 slab models, and in the CFMIP-2 experiments. The cloud feedbacks in the CMIP3/CFMIP-1, amip4K and amipFuture ensembles, and the cloud adjustments in the amip4xCO<sub>2</sub> ensemble all show large standard deviations in the subtropical stratocumulus and trade cumulus regions, underscoring the dominant contribution of low clouds to inter-model spread in cloud feedback and cloud adjustment in these experiments, consistent with the findings from the coupled models. Figure 3 also clearly shows the dominant role of the tropics in inter-model spread in cloud feedback and adjustment. The inter-model variance in the cloud feedbacks and cloud adjustments were also decomposed into contributions from cloud feedback regimes dominated by low and high cloud and low level cloud changes, following the method of Webb et al. (2006). These results are summarised in Figure 4, and highlight again the dominant role played by low clouds in inter-model spread in cloud feedback and cloud adjustment. (Details of the decomposition method can be found in deliverable D2.7.)

As mentioned above, the CFMIP-2 experiments also include process level outputs, including high frequency outputs at selected gridpoints. These have been analysed as part of WP3 (see deliverable D3.8). Webb et al. (submitted) used these data to resolve the cloud feedbacks in a subset of the CFMIP-2 models into contributions from different times of the day, and from occasions when low level clouds are dominant. They found that the models tend to show larger changes in low cloud properties in the warmer climate in the morning when more low cloud is present in the control. This results in shortwave cloud feedbacks being strongest and having the largest inter-model spread at this time of day. They also found that most of the inter-model spread in the diurnal mean marine shortwave cloud feedback can be explained by low cloud responses, although these do not explain so well the model responses at the neutral/weakly negative end of the feedback range, where changes in mid and high level cloud properties are more important (see Figure 5).

Finally, the analysis of Webb et al. (2013) (which composited tropical marine cloud feedbacks and adjustments in the CMIP3/CFMIP-1 experiments into equally populated percentile ranges of lower tropospheric stability (LTS)) has been repeated for the CFMIP-2 amip4K experiments (Figure 6). The largest inter-model spread in net cloud feedback is found in the most stable regimes in the 60-100% LTS percentile range, and is strongly correlated with the shortwave cloud feedback in this regime, where shallow clouds predominate, consistent with the findings from Webb et al.

(2013) for the CFMIP-2/CMIP3 slab models and Vial et al. (2013) for the CMIP5 coupled models.

Overall, work under WP2 has shown that several lines of evidence support the conclusion that that subtropical shallow cloud regimes continue play in a leading role in cloud feedback uncertainty.

### **3. Interpretation of inter-model spread in GCM cloud feedback based on SCM, LES and MLM results.**

Given that the largest source of uncertainty in cloud climate feedback in ESM's arises in subtropical shallow cloud regimes, work on cloud feedbacks in WP3 has concentrated on stratocumulus and shallow cumulus cloud regimes.

The approach of WP3 has been to understand cloud feedback mechanisms in idealised experiments using a combination of different types of models:

1. Large Eddy Simulations were used to establish the most reliable and most realistic estimates for the representation of stratocumulus cumulus and transitions between these regimes both in present and future climate conditions.

2. Simple idealised Mixed Layer Models of the subtropical atmospheric boundary layer were used to interpret the behaviour of the realistic but complex results from the Large Eddy Simulations.

3. Single Column Models were used to assess the extent to which the parameterization packages in the ESM's are capable of reproducing the responses that are found for the Large Eddy Simulations when subjected to the same large scale forcings and perturbations.

The cloud feedback work in WP3 has fallen under two broad initiatives. The first uses the framework of the CGILS project (CFMIP-GASS Intercomparison of Large-Eddy and Single- Column Models, Zhang et al. 2012), an international effort compare cloud feedbacks in SCMs and LES in an idealised cloud feedback case, based on the GCSS Pacific Cross Section which originated in a previous European FP5 project EUROCS. ESM outputs for different periods along this transect have been reported in the literature (Siebesma et al. 2004, Teixeira et al. 2011) and provided the basis for three CGILS cases representing solid stratocumulus (S12), cumulus under stratocumulus (S11) and Shallow Cumulus (S6) (Figure 7). These are subjected to idealized future climate conditions in order to determine the cloud-radiative feedback by increasing the SST by 2K and through weakening the imposed subsidence (Zhang and Bretherton, 2008, Zhang et al. 2012). More details on this work are provided in Deliverable 3.9. The second initiative extends the CGILS framework into a two dimensional phase space with dimensions of lower tropospheric stability (LTS) and free tropospheric humidity. More details of this work may be found in deliverable 3.5. We now summarise the main findings from these two initiatives and use them to interpret the GCM results.

#### *3.1 Interpretation of inter-model spread in GCM cloud feedback based on CGILS results.*

Zhang et al. (2013) reported results from the first phase of CGILS. The CGILS SCMs differ greatly in their cloud feedbacks with both positive and negative net CRE responses in all three regimes (see Figures 8, 9). The LES results tend to show smaller ranges, with mostly positive values at s6 and s11, but mostly negative values at s12 (Figure 10).

The SCM feedbacks at s12 range from -12 to 16  $\text{Wm}^{-2}\text{K}^{-1}$ , with a median value of 0, while those at s11 range from -8 to 13  $\text{Wm}^{-2}\text{K}^{-1}$  with a median value of 0.5. This range is much larger and more symmetric about zero than is the case for the GCMs responses at the stable end of the LTS range, which range from -0.2 to 3.2  $\text{Wm}^{-2}\text{K}^{-1}$  with a median of 1.2 (Figure 6). The SCM feedbacks at s6 range from -7 to 9  $\text{Wm}^{-2}\text{K}^{-1}$ , with a median value of -0.1. This range is again much larger than that from the GCMs in the mid-LTS range; for example the range in the net CRE response in the 50-60% range of LTS is -0.8 to 0.8  $\text{Wm}^{-2}\text{K}^{-1}$ , with a median of 0.3. The s6 SCM results and GCM results in the mid-LTS range are however quite equally distributed between positive and negative values. Figures 8 and 9 also show that the models that have active shallow convection in the control state are more likely to have positive feedbacks, while the remaining models more often have negative feedbacks. Zhang et al. (2013) argue that, in the absence active shallow convection, increasing surface fluxes moisten the boundary layer and increase low cloudiness in the SCMs, resulting in a negative cloud feedback. However, when shallow convection is active it entrains additional warm, dry air into the boundary layer in the warmer climate, resulting in a positive feedback. Differences in the relative strengths of such competing mechanisms can subsequently result in a range of positive and negative cloud feedbacks across the SCMs.

The LES models exhibit a smaller range of feedbacks than the SCMs, and are mostly positive at s11, ranging from -0.5 to 5  $\text{Wm}^{-2}\text{K}^{-1}$  with a median of 3  $\text{Wm}^{-2}\text{K}^{-1}$ , but mostly negative at s12, ranging from -8 to 5  $\text{Wm}^{-2}\text{K}^{-1}$  with a median of -6  $\text{Wm}^{-2}\text{K}^{-1}$ . The s6 results are systematically weakly positive and show a very narrow range of 0.5-1  $\text{Wm}^{-2}\text{K}^{-1}$  with a median of 0.5. The mechanisms underlying the LES results for CGILS are reported in detail by Blossey et al. (2012). All LES models simulate boundary-layer deepening due to reduced subsidence in the warmer climate, with less deepening at s6 due to regulation by precipitation. The majority predict cloud thickening s12 and a slight cloud thinning at s11 and s6. In perturbed climate simulations at s12 without the subsidence decrease, liquid water path (LWP) consistently decreases across the LES models.

Comparison of the CGILS SCM and LES results provides a benchmark for testing SCM physics, albeit in an idealised framework. Comparison of the median responses of the LES and SCM results indicates that the SCM feedbacks tend to be positively biased at s12, negatively biased at s11, but relatively unbiased at s6. SCMs with active shallow convection at s11 tend to reproduce the positive feedback seen in the LES models at that location, while SCMs which rely solely on turbulent mixing tend to agree better with the negative feedback seen in the LES models at s12. This suggests that varying levels of skill shown by the SCMs in discriminating between turbulently and convectively mixed boundary layers are relevant to the strength and even the sign of their cloud feedbacks.

As noted above, CGILS SCM and LES results exhibit a range of feedbacks larger than that seen in the GCM composites. There are a number of reasons why we would expect this. First, the GCM composites average together many regimes with varying amounts of cloud, many of which will be less than those present along the GPCI, which was defined to pass through the Californian stratocumulus deck. In contrast, CGILS forces the SCMs and LES models with a steady state forcing which in the case of s11 and s12 reproduces a persistent unbroken stratocumulus deck with no synoptic variability. This is expected to result in stronger feedbacks in the SCMs. Second, CGILS focuses on July, the time of year when the CGILS regimes are subject to maximum insolation. Third, CGILS forces the SCMs with a constant diurnal mean

insolation value. The GCMs exhibit a diurnal cycle in low level clouds over the oceans which results in them having less low level cloud at noon than during the night, and this effect may well contribute to weaker shortwave cloud feedbacks in the GCMs compared to the SCMs.

There is no particular reason however to expect that these effects would explain the tendency for the GCMs to show more positive feedbacks in stable regimes than is seen in the SCMs at s11/s12. We now consider whether this difference might be caused by differences in the large scale forcings in the GCM and SCMs at s11/s12.

First, we consider changes in LTS with the warmer climate. In the CGILS case, LTS increases by 0.7K/K at s11 and s12. Increases in LTS (in the absence of other changes) are expected to result in an increase in cloud fraction as the strength of the inversion increases, reducing mixing across the inversion and increasing relative humidity in the boundary layer. In the GCMs, LTS increases by 0.3-0.6K/K in the most stable LTS bin, with a median increase of 0.5K/K (Figure 12). The stronger increases in LTS in the CGILS case at s11 and s12 compared to that seen in the GCMs may therefore contribute to the tendency for more negative feedbacks in the SCMs.

Second, in CGILS at s11 and s12, subsidence (as measured by 500mb pressure velocity) weakens by 2 and 3hPa/day/K respectively, while the GCMs ensemble mean subsidence weakens by just 0.8-1.7hPa/day/K in the most stable LTS bin, with a median reduction of 1.2 (Figure 12). The stronger subsidence weakening in CGILS could possibly result in a deepening of the boundary layer, a thickening of the cloud layer and an increase in liquid water path in the SCMs. A sensitivity test in which the s12 LES case was repeated with no reduction in subsidence showed a less negative cloud feedback, so a similar sensitivity to the subsidence weakening in the SCMs and GCMs would be expected to contribute to the feedbacks being more negative in the SCMs.

Finally, we consider the role that surface evaporation might play in the differing responses of the SCMs and GCMs. In the absence of changes in near-surface relative humidity, air-sea temperature differences or surface wind speed, surface evaporation over the ocean is expected to increase by 7%/K (Rieck et al. 2012). This translates to an increase in surface latent heat flux of around  $6 \text{ Wm}^{-2}\text{K}^{-1}$  in regimes like s11 and s12, but in fact evaporation increases by considerably less than this, because of a weakening of the overturning circulation, reduced surface winds and air-sea temperature differences and increases in near-surface relative humidity (Richter and Xie (2008), Webb and Lock (2013)). In the most stable LTS regimes the GCMs show increases in surface latent heat flux ranging from of  $1.8\text{-}4.0 \text{ Wm}^{-2}\text{K}^{-1}$  with a median value of 3.5 (Figure 12). At s11, the SCMs show increases ranging from  $2.5\text{-}12.5 \text{ Wm}^{-2}\text{K}^{-1}$  (Figure 11), with a median value of 3.5. Given the similar median responses between the SCMs and the GCMs, we consider it unlikely that differences in surface evaporation contribute substantially to the tendency for more negative cloud feedbacks in the SCMs.

Given these differences, it is difficult to interpret the GCM feedbacks quantitatively in terms of the CGILS SCM and LES results. On the basis of the SCM/LES comparison, one could argue that the GCM feedbacks should on average be more negative in stratocumulus regimes like those simulated at s12, but more positive in regimes where stratocumulus is fed by shallow cumulus, as at s11. However, we do not at present have a way to assess the impact of this on the overall feedbacks in the GCMs, as it is not currently straightforward to separate these regimes in the GCMs. Overall we conclude that the CGILS results show no clear evidence of

a systematic bias in cloud feedback in the GCMs. However the large range of SCM feedbacks compared to the equivalently forced the LES experiments suggests that errors in the responses of the local physics contribute substantially to inter-model spread in cloud feedback in the GCMs. Hence the prospect of improving the performance of future parametrizations by comparing SCMs with LES models in the CGILS framework is promising.

### *3.2 Interpretation of inter-model spread in GCM cloud feedback based on phase space results.*

The second initiative within WP3 extends the CGILS experiments into a two dimensional phase space as described in De Roode et al. (submitted). This simulates stratocumulus equilibrium states using a mixed-layer model of the boundary layer in a two dimensional phase space with axes of LTS and free troposphere humidity at 700hPa. In contrast to CGILS, the LWP response is examined by perturbing various cloud-controlling-factors in turn. To clarify the role of changes in cloud top entrainment, this is done first with fixed entrainment, and again allowing entrainment to respond to the other cloud controlling factors.

Figure 13 shows the LWP response to changes in the potential sea surface temperature  $\theta_0$ , the free tropospheric potential temperature  $\theta_{ft}$ , the free tropospheric specific humidity  $q_{ft}$ , and the horizontal wind speed for fixed entrainment. Surface warming increases surface evaporation and boundary layer relative humidity, lowering the cloud base and increasing the LWP. Increasing surface wind speed also acts to increase surface evaporation and hence LWP, consistent with earlier findings by Webb and Lock (2013) and Bretherton et al. (2013). Warming the free troposphere reduces the relative humidity of the air which is entrained into the boundary layer from above, increasing cloud base height and reducing LWP. Moistening the free troposphere in absolute terms has the opposite effect, increasing the LWP. The latter effect would be expected to outweigh that of the reduction due to free tropospheric warming if the specific humidity increase was large enough to result in an increase in relative humidity.

Figure 14 shows the LWP responses when entrainment is allowed to respond. The responses to changes in free tropospheric humidity and surface winds are comparable with and without fixed entrainment. Increases in surface temperature weaken the inversion, increasing entrainment of warm, dry air from above, reducing relative humidity, and raising cloud base. In the lower right quadrant of the phase space the free troposphere is sufficiently warm and dry that the additional entrainment raises the cloud base more than the cloud top, acting to thin the cloud layer and reduce LWP, eventually overcoming the effect of increasing surface evaporation. Similarly increases in free tropospheric temperature strengthen the inversion, reducing entrainment and thickening the cloud. Again this has the largest effect when the free troposphere is warmest and driest. With interactive entrainment it is also possible to test the sensitivity increasing subsidence/horizontal divergence; this results in a thinning of the cloud and reduction in LWP as the boundary layer becomes shallower, consistent with the CGILS LES results.

Subsequent work in WP3 by Dal Gesso et al (2013) has modified the MLM to allow for the effect of increasing free tropospheric humidity on the downwelling longwave radiation, which reduces the radiative cooling of the boundary layer and the entrainment rate. The reduced entrainment was found to reduce the depth of the boundary layer, while the reduced radiative cooling was found to reduce relative

humidity, raising cloud base and reducing LWP, consistent with the findings of Bretherton et al. (2013).

Turning again to the GCMs, Figure 6 shows that in the most stable LTS regime, cloud fraction and LWP decreases in most models resulting in a largely positive shortwave cloud feedback. The LWP responses in the GCMs are however much smaller than those in the MLM, presumably because the MLM represents a solid sheet of persistent stratocumulus with no synoptic variability. In the most stable LTS bin, the GCMs have time mean control values of LTS ranging from 18.5-20K, and values of  $q_{ft}$  ranging from 0.2-0.3 g/kg (not shown). This would place the GCMs on average near the lower left corner of the phase space in Figures 13 and 14 (although of course instantaneous values would explore a wider range).

In the most stable LTS bin the GCMs tend to show reductions in subsidence and increases in LTS and free tropospheric relative humidity (Figure 12). The MLM results from De Roode et al. (submitted) would predict an increase in LWP if only these conditions are changed. However, an increase in the specific humidity will increase the amount of downwelling radiation such that the longwave radiative cooling at the cloud top will be reduced. This effect tends to diminish the entrainment rate which subsequently leads to a smaller LWP. The MLM study by Dal Gesso et al (2013) takes into account both the changes in the free troposphere and the radiative forcing and find that for a perturbed climate the LWP reduces. The GCMs do also exhibit a systematic reduction in near-surface wind speed (not shown), for which the MLM results predict a thinning of the cloud and a reduction in LWP.

Dal Gesso et al. (submitted) have repeated the phase space study with the EC-EARTH SCM, with both constant and large-scale forcing conditions. For constant forcing, most of the simulations reached a steady state, yet in a few runs significant and persistent temporal variations in the boundary layer state were found. With stochastic forcing in the large-scale subsidence, the cloud-top height showed a relatively small sensitivity to the LTS, whereas the free tropospheric humidity strongly controls both cloud base and top heights. By contrast, the transition of a stratocumulus cloud deck with a cloud cover of unity to a broken cloud field appeared to be controlled mainly by the LTS. High LWP values are predominantly found for high LTS values, although an area with enhanced LWP values are also found for an LTS of about 18 K. Figure 15 shows the response of the boundary layer depth, cloud cover and LWP to changes in the SST for the EC-Earth SCM. For these perturbed climate simulations the free tropospheric relative humidity and the LTS were kept the same as in the control case. The runs with the stochastic forcing exhibit a distinct decrease in both the cloud cover and the LWP. Figure 16 shows qualitatively similar results with a positive shortwave cloud feedback, a reduction in LWP and cloud fraction which is broadly consistent with that seen in the full GCM (Figure 6). This demonstrates that the phase space approach is able to reproduce key aspects of the full GCM response once stochastic forcing is applied.

There is still considerable uncertainty over the processes which control turbulent cloud top entrainment, and so its treatment in turbulent mixing schemes in GCMs is necessarily incomplete. However, the GCMs lie on average in a regime where the MLM predicts that increases in turbulently driven entrainment will not reduce LWP substantially in the warmer climate, so this failing may not affect their cloud feedbacks substantially. However, as pointed out by Zhang et al. (2013), many of the CGILS SCMs do show evidence of enhanced entrainment of free tropospheric air into boundary layer in the warmer climate, not through turbulent mixing, but through entrainment which occurs through compensating subsidence when shallow

convection penetrates the inversion. The MLM results highlight the potential impact of changes in entrainment on cloud feedback, clearly demonstrating its ability to change the sign of the LWP response. They also demonstrate that the sign of the response to the same climate change forcing can be positive or negative depending on the control state. This underscores the importance of testing the sensitivity to and improving the representation of entrainment processes, as well as reducing biases in the simulation of present-day subtropical clouds in GCMs.

It should also be noted that most GCMs do not have sufficient vertical resolution to resolve the relatively subtle changes in cloud thickness and LWP predicted by the LES and MLM results. Coarse vertical resolution could result in GCMs responding to changes a drying of the boundary layer by reducing cloud fraction when they should maintain cloud fraction with a thinner cloud, distorting the cloud feedback response. Improved vertical resolution in the boundary layer would seem to be a necessary requirement for improved confidence in SCM and GCM cloud feedbacks.

#### **4. Interpretation of inter-model spread in GCM cloud feedback based on sensitivity experiments.**

WP4, entitled “Sensitivity experiments and hypothesis testing” has been responsible for developing physical hypotheses relating to cloud feedback mechanisms, and testing them by performing sensitivity experiments with the GCMs. In many cases, the physical hypotheses tested have been developed based on the findings from SCM, LES and MLM experiments; however hypotheses arising from analysis of the GCMs have also been tested, recognising the fact that there may be factors affecting the feedbacks in the full GCMs which are not captured by idealised scenarios used to force the MLM, SCM and LES models.

##### *4.1 Interpretation of inter-model spread in GCM cloud feedback based on parameter sensitivities.*

Initial work in WP4 reviewed sensitivity experiments based on parameter perturbations, and this is reported in deliverable report D4.1. Controls on climate sensitivity have been explored using multi-model ensembles (MME) and perturbed parameter ensembles (PPE) by a number of groups. For example, Webb et al. (2013) found a very strong relationship between biases in cloud radiative effect, or net top-of-atmosphere radiation, and the climate sensitivity across their PPE. This relationship was not however reproduced within the CMIP3 MME. Similarly, using a PPE derived from a different model, Klocke et al. (2011) found that climate sensitivity is well correlated with root-mean-square errors in cloud-radiative effects in strongly subsiding regions characterized by intermediate values of lower tropospheric stability. However this property of the PPE also did not explain differences in the climate sensitivity of the CMIP3 MME. Brient and Bony (2012) explored a limited PPE using the IPSL model, and in so doing also showed that factors which tended to increase low cloud amount, for instance a change in the formulation of their statistical cloud scheme or a change in their precipitation efficiency, also increased the sensitivity of low clouds to changing surface temperatures. A general finding has been that relationships that emerge from the PPE framework do not generalize to the MME. For this reason, subsequent work under WP4 has focused more on ‘structural’ sensitivity tests, in which feedback loops are cut by suppressing different processes in turn.

#### *4.2 Sensitivity tests in individual models.*

Brient and Bony (2013) argued that cloud feedbacks in GCMs can be understood in terms of the moist static energy (MSE) budget of the atmosphere. As the climate warms, changes in surface fluxes and clear-sky radiative cooling perturb the MSE budget of the atmosphere, creating an energetic imbalance which is restored primarily by changes in cloudiness via longwave cloud cooling. They examined cloud feedbacks in IPSL-CM5A-LR, and argued that in the warmer climate, increases in surface fluxes in this model resulted in a deepening of the boundary layer, and a reduction in the vertical gradient of the moist static energy (MSE) between the boundary layer and the free troposphere in the subtropics. However, the Clausius Clapeyron relation acted to oppose this effect, increasing the overall vertical MSE gradient, the strength of the vertical MSE advection and the import of low-MSE air into the boundary layer in the warmer climate. They performed a number of sensitivity experiments, and found a strong relationship between the change in the vertical advection of the MSE and the low-level cloud change in their model, arguing that the enhanced vertical advection of low MSE air into the boundary layer makes the MSE sink from cloud radiative cooling less necessary to balance the MSE budget, resulting in decreases in low-level cloud fraction.

Subsequently, Brient and Bony (2012) argued that the size of the cloud change in response to a perturbation of the MSE budget is determined by the strength of the coupling between cloud properties and the longwave cloud radiative cooling. They tested this idea by performing sensitivity tests in which the longwave radiative cooling associated with clouds was scaled by a 'beta' parameter. For the case  $\beta=0$ , where changes in cloudiness do not affect the MSE budget, the cloud response to the warming climate was found to be greatly reduced. This result suggests that the radiative cooling rate of clouds in the control state can be proportional to the change in this quantity under climate change, which may explain the relationship between present day cloud fraction and cloud fraction response in this model noted in the previous section.

Webb and Lock (2013) tested a number of hypothesised cloud feedback mechanisms by performing sensitivity tests in HadGEM2-A, which also has substantial positive cloud feedbacks in the subtropical stratocumulus/trade cumulus transition regions associated with reductions in boundary layer cloud fraction. Applying the MSE budget approach of Brient and Bony (2013) to HadGEM2-A over the subtropical Northeast Pacific established that although stronger vertical advection of MSE does enhance the rate of MSE depletion from the boundary layer in this model, this effect can explain only a small fraction of the cloud MSE response and hence the cloud feedback. Other terms, including turbulent mixing forced by surface fluxes make larger contributions to the perturbed MSE budget which are comparable in magnitude to the cloud MSE response term.

Webb and Lock (2013) also found that reductions in near-surface wind speed and air-sea temperature differences combined with increases in near-surface relative humidity limited increases in surface evaporation to just  $3 \text{ W/m}^2$  or  $0.6 \text{ \%/K}$  in HadGEM2-A. Previous studies such as Rieck et al. (2012) have suggested that increases in surface evaporation may be required to maintain maritime boundary layer cloud in a warmer climate. This suggests that the supply of water vapour from surface evaporation in HadGEM2-A may not be increasing enough to maintain the relative humidity of the boundary layer and hence the low level cloud fraction in the warmer

climate. This hypothesis was tested by forcing the surface evaporation to increase more rapidly in the GCM; this yielded a substantially weaker cloud feedback, supporting the hypothesis. A tendency for the turbulent mixing profiles to become more ‘bottom heavy’ in the warmer climate, reducing the moisture supply to the cloud layer was also noted. Such a weakening of the vertical mixing by the boundary layer scheme might be explained by the reduction in surface wind speed and an associated reduction in the surface sensible heat flux.

Examination of the surface fluxes in the CMIP5 GCMs shows reductions in sensible heat flux in the warmer climate, and relatively weak increases in surface latent heat flux in the more stable LTS regimes (Figure 12). These are caused by reductions in air-sea temperature differences and near-surface wind speed, and increases in near-surface relative humidity (not shown), as found by previous studies. The relatively weak increases in surface evaporation in particular could explain the tendency for models to show positive cloud feedbacks in the more stable regimes; however changes in surface fluxes are not correlated with cloud feedback across the models, so we have no evidence to support them being a dominant driver of the inter-model spread.

Figure 12 also shows changes in boundary layer depth (as diagnosed by the difference between the surface pressure and the pressure at the level where relative humidity drops below 50%). This increases in most models, particularly in the more stable regimes, as predicted by Rieck et al. (2012) and Brient and Bony (2013) in response to the increasing surface latent heat flux. This deepening is consistent with enhanced entrainment at the top of the boundary layer via shallow convection, as argued by Zhang et al (2013).

#### *4.3 Coordinated sensitivity tests across models.*

WP4 has also organised two sets of coordinated sensitivity tests with multiple models. The Clouds On/Off Climate Intercomparison Experiment (COOKIE) repeated amip, amip4K and amip4xCO<sub>2</sub> experiments and aquaplanet equivalents but with clouds made transparent to radiation, repeating the beta=0 experiment of Brient and Bony (2012). These experiments also allow the effects of clouds and cloud changes on other aspects of the climate system (such as regional warming and precipitation changes) to be quantified. The Selected Process On/Off Climate Intercomparison Experiment (SPOOKIE) is a newer initiative from WP4 which aims to establish the relative contributions of different areas of model physics to inter-model spread in cloud feedback by switching off or simplifying different model schemes in turn. A pilot experiment following the SPOOKIE approach is currently underway and initial results are reported below.

The initial SPOOKIE pilot experiments have focused on convective parametrization, for a number of reasons. First, a number of studies (e.g. Brient and Bony 2013) have suggested that changes in deep convection in the warming climate might have a remote influence on subtropical cloud feedbacks, via their impact on the circulation and temperature and humidity structure of the tropical free troposphere. Moreover, differences in convective parametrizations in models might explain some of the inter-model differences in these large scale responses and hence some of the inter-model spread in cloud feedback. Second, the results from CGILS outlined in the previous section suggest that the ability of the SCMs to correctly diagnose the presence of convection has a substantial impact on cloud feedback. More specifically, Zhang et al. (2013) identify enhanced boundary layer entrainment associated with

shallow convection as a key driver of positive subtropical cloud feedback in the CGILS SCMs. Third, recent work by Sherwood et al. (2014) has argued that a substantial fraction of the variation in the strength of low level cloud feedback across models is regulated by the strength of mixing between low and mid levels by convection and the large-scale shallow overturning circulation in the present day climate. This controls the degree to which the boundary layer dries and low cloud reduces as the climate warms. They show that indirect observable proxies for the lower tropospheric mixing rate based on the tropical temperature, humidity and vertical velocity show significant correlations with ECS and cloud feedback, statistically ‘explaining’ just under half of the inter-model variance in the ECS. Comparisons with observations suggest that the more realistic models have stronger lower tropospheric mixing, more positive low level cloud feedbacks and climate sensitivities above 3K.

Motivated in part by these findings, the pilot SPOOKIE experiments have repeated the CFMIP-2/CMIP5 amip/amip4K experiments with convective parametrization turned off. In these experiments (convoffamip and convoffamip4K), instability which would be removed by the convection scheme is instead removed by the turbulent mixing schemes and the large scale dynamics. If the details of deep convective parametrization are indeed responsible for a substantial part of the inter-model spread in cloud feedback, then these experiments might be expected to exhibit a narrower range of cloud feedback. Equally, if parametrized shallow convection is responsible for positive subtropical cloud feedbacks in the GCMs, as suggested by Zhang et al. (2013), then the convoff experiments will have neutral or negative cloud feedbacks.

Figure 17 shows net, SW and LW CRE responses for the amip/amip4K and convoffamip/convoff4K experiments from the models participating in the SPOOKIE pilot study, composited into equally sized LTS percentile bins over the tropical oceans as in Figure 6. The standard experiments with the four participating models cover a substantial fraction of the overall inter-model range (compare Figures 6 and 15), although the participation of IPSL\_CM5A\_LR and CNRM\_CM5 which is planned will cover this range more completely. It is also encouraging that the correlation between the net and SW CRE responses in the stable LTS bins is reproduced with just these four models.

Figure 17 additionally shows that the convoff experiments exhibit a strong convergence in the character of the tropical cloud feedback compared to the versions with parametrized convection. The net cloud feedback shows a reduced or similar spread across the regimes, and a relatively smooth and monotonic transition from positive feedback in stable regimes to weakly negative feedback in unstable regimes. What spread there is in the net is now mostly due to the shortwave component, and the two are now correlated across all regimes. This is in part due a strong convergence in the longwave CRE response in the convoff experiments and a reduction in the magnitude of opposing longwave and shortwave responses in the more unstable regimes. This convergence is also reflected in the range of the global mean net cloud feedback, which is reduced by 43% from [-0.22 to 0.25] in the amip/amip4K experiments to [0.02 to 0.18] in convoffamip/convoffmip4K.

Figure 18 shows that the cloud fraction response has a smaller spread and is more consistent across regimes in the absence of parametrized convection, while the spread in the LWP and IWP responses is not greatly affected. This, coupled with the strong convergence in the cloud feedback, confirms that the differing cloud fraction responses are the dominant drivers of cloud feedback spread across the low latitude

oceans in these models, and that much of this is caused by differences in parametrized convection. It can be argued that substantial changes in cloud fraction will generally require changes in relative humidity, and that parametrized convection is more easily able to change relative humidity than other vertical mixing schemes. This is because parametrized convection is able to transport humidity over the full depth of the troposphere in a single time step, while the large scale dynamics and turbulent mixing schemes transport humidity more gradually, often responding mainly to local vertical gradients in moist conserved variables.

Figure 19 shows that the equivalent responses in LTS and 700mb relative humidity also show a considerable convergence in the convoff experiments. The unusual responses in LTS and free tropospheric relative humidity in MIROC5 are not present in the convoff experiments, indicating that these are related to the response of the MIROC5 convection scheme. This behaviour may be related to improvements to the MIROC convection scheme which allow the lateral entrainment rate to vary depending on the humidity of the free troposphere, increasing detrainment in the mid-troposphere and improving various aspects of present day simulation (Chikira and Sugiyama 2010). The response of the subsidence rate also converges somewhat when convective parametrization is switched off. The subsidence rate still weakens in the most stable regimes however, indicating that this aspect of the model response is not a function of convective parametrization. The free tropospheric relative humidity also continues to rise in these regimes.

Figure 20 shows that there is also a certain degree of convergence in the responses of the latent heat fluxes in the convoff experiments, but this is not the case for the sensible heat fluxes. This is mainly due to more consistent responses in near-surface relative humidity rather than in near-surface wind speed or air sea temperature difference (not shown), and suggests that differences in the details of convective parametrization schemes are leading to different responses in boundary layer relative humidity. Additionally, the increases in boundary layer depth typically seen in the versions of the models with parametrized convection are largely absent in the convoff experiments in the 50-100% LTS percentile range (Figure 20). This suggests that the deepening of the boundary layer seen in GCMs in the warmer climate is generally a consequence of increased boundary layer entrainment by parametrized convection. In the absence of convection, the boundary layer depth generally decreases in the warmer climate, consistent with the expectation from the MLM results that turbulent entrainment will reduce with a strengthening of the inversion.

Overall, the convoff pilot experiments indicate that differences in the parametrized convection responses in the models do indeed contribute substantially inter-model spread in both deep convective and subtropical cloud feedbacks, consistent with the expectation from Zhang et al. (2013) and Sherwood et al. (2014). Although the response of the free troposphere is also affected, this is less the case in the subtropics than in the deep convective regions, so these experiments do not provide clear evidence of a remote control of deep convection on subtropical cloud feedback. The presence of positive subtropical feedbacks in the absence of parametrized convection (albeit with reduced inter-model spread) does indicate however that processes other than shallow convective entrainment are contributing. The relatively weak increases in surface evaporation in the most stable regimes are still present, and so remain as a potential explanation for the generally positive subtropical cloud feedback in the GCMs. Another possibility is the Entrainment Liquid Flux (ELF) mechanism demonstrated in a recent LES study by Bretherton and Blossey (2014), where an increased cloud layer humidity flux in a warmer climate

induces an entrainment liquid-flux adjustment that dries the stratocumulus cloud layer. Alternatively, the large scale component of the lower tropospheric mixing mechanism proposed by Sherwood et al. (2014) could be responsible. We plan to develop the SPOOKIE approach further in the future by designing sensitivity tests for GCMs which target such remaining questions more directly.

## 5. Summary and Conclusions

One of the central aims of EUCLIPSE has been to improve our physical understanding of how cloud processes respond to and feedback on climate change, and of the reasons for inter-model differences in these cloud feedbacks. Here we have reviewed the results from work packages 2, 3 and 4 relevant to interpreting the inter-model differences in cloud feedback in the CMIP5 models.

WP2, entitled “Climate Model Evaluation and Analysis” has been (amongst other things) responsible for quantifying and interpreting the inter-model spread of climate sensitivity and cloud feedback from the models. This has included identifying the regions, the cloud regimes and the meteorological conditions primarily responsible for this spread, and exploring the mechanisms that control the different model responses. The range of equilibrium climate sensitivity in the CMIP5 AOGCMs was found to be 2.1-4.7K, similar to that derived from CMIP3 models (2.1-4.4K), and differences in cloud feedbacks have been shown to make the largest contribution to this range, as previously. The regions, cloud regimes and meteorological conditions responsible for the spread in cloud responses in the models were examined in a number of ways. Inter-model differences in tropical cloud feedbacks were found to contribute more than twice as much as the higher latitude regions to the spread in cloud feedback in the CMIP5 coupled models. Thermodynamic components of the cloud feedback showed largest differences between low and high sensitivity models in regions of weak-moderate subsidence, where shallow clouds such as stratocumulus and trade cumulus predominate. Cloud feedbacks in the CFMIP-2/CMIP5 amip4K and amipFuture experiments all showed large inter-model standard deviations in the subtropical stratocumulus and trade cumulus regions, and in regimes of strong stability, consistent with the findings from the coupled models.

WP3, entitled “Process Level Evaluation” has been responsible for understanding the processes underlying the responses of boundary layer clouds in idealised and future climate conditions, through the use of LES (Large Eddy Simulation) models, idealised simple models such as boundary layer mixed layer models (MLMs) and Single Column Model (SCM) versions of the GCMs.

The CGILS SCMs differ greatly in their cloud feedbacks with both positive and negative net CRE responses for all three regimes (solid stratocumulus s12, cumulus under stratocumulus s11 and shallow cumulus s6). In the absence active shallow convection, increasing surface fluxes moisten the boundary layer and increase low cloudiness, resulting in a negative cloud feedback. However, when active, shallow convection can entrain additional warm, dry air into the boundary layer in the warmer climate, resulting in a positive feedback. Models which have active shallow convection in the control state are more likely to have positive feedbacks while the remaining models more often have negative feedbacks.

The LES results tend to show smaller ranges, with mostly positive values as s6 and s11, but mostly negative values at s12. All LES models simulate boundary-layer deepening due to reduced subsidence in the warmer climate, with less deepening at s6 due to regulation by precipitation. The majority predict cloud thickening at s12 and a

slight cloud thinning at s11 and s6. In perturbed climate simulations at s12 without the subsidence decrease, LWP consistently decreases across the LES models.

Comparison of the CGILS SCM and LES results provides a benchmark for testing SCM physics, albeit in an idealised framework. Compared to the LES models, SCM feedbacks tend to be positively biased at s12, negatively biased at s11, but relatively unbiased at s6. SCMs with active shallow convection at s11 tend to reproduce the positive feedback seen in the LES models at that location, while SCMs which rely solely on turbulent mixing tend to agree better with the negative feedback seen in the LES models at s12. This suggests that varying levels of skill shown by the SCMs in discriminating between turbulently and convectively mixed boundary layers are relevant to the strength and even the sign of their cloud feedbacks.

The CGILS SCM and LES results exhibit a range of feedbacks larger than that seen in the GCMs. This it be expected, given that the GCMs incorporate diurnal and synoptic variability, while the SCMs and LES models are largely subject to a steady state forcing which in the case of s11 and s12 reproduces a persistent unbroken stratocumulus deck with no synoptic variability. Additionally, the GCMs tend to show more positive feedbacks in stable regimes than are seen in the SCMs at s11/s12. Comparison of large scale forcings indicates that a stronger increase in lower tropospheric stability and a stronger weakening of subsidence in the CGILS forcing compared to that typically seen in the GCMs contribute to this difference. Given these differences, it is difficult to interpret the GCM feedbacks quantitatively in terms of the CGILS SCM and LES results. Overall we conclude that the CGILS results show no clear evidence of a systematic bias in cloud feedback in the GCMs. However the large range of SCM feedbacks compared to the equivalently forced the LES experiments suggests that errors in the responses of the local physics contribute substantially to inter-model spread in cloud feedback in the GCMs. Hence the prospect of improving the performance of future parametrizations by comparing SCMs with LES models in the CGILS framework is promising.

The second initiative of WP3 extends the CGILS approach into a broadened two dimensional phase space with axes of lower tropospheric stability and free troposphere humidity at 700hPa. The LWP response was investigated by perturbing various cloud-controlling-factors in turn in an idealised mixed layer model (MLM) of the boundary layer. To clarify the role of changes in cloud top entrainment, this was done first with fixed entrainment, and again allowing entrainment to respond to changes in the other cloud controlling factors. Surface warming was found to increase surface evaporation and boundary layer relative humidity, lowering the cloud base and increasing the LWP. Warming the free troposphere reduced the relative humidity of the air which is entrained into the boundary layer from above, increasing cloud base height and reducing LWP. When entrainment was allowed to respond to large scale forcings, increasing surface temperature weakened the inversion, increasing entrainment of warm, dry air from above, reducing the relative humidity of the boundary layer, and raising cloud base. Similarly increases in free tropospheric temperature strengthened the inversion, reducing entrainment and thickening the cloud. Where the free troposphere is relatively warm and dry in the control climate, the impact of changes in entrainment can be large enough to change the sign of the LWP response. Reducing surface wind speed acts to reduce surface evaporation and hence LWP. Additionally, allowing for the effect of increasing free tropospheric humidity on the downwelling longwave radiation showed a reduction in the radiative cooling of the boundary layer and the entrainment rate, the net effect of which was to

reduce the relative humidity of the boundary layer, raising cloud base and reducing LWP.

In the stable regimes in the GCMs, cloud fraction and LWP decreases in most models resulting in a largely positive shortwave cloud feedback. The GCMs show a reduction in wind speed, for which the MLM results predict a thinning of the cloud and a reduction in LWP. Specific humidity increases in the free troposphere in the GCMs, which is also predicted to reduce LWP in the MLM. Therefore the MLM results suggest these large scale forcings as potential candidates for explaining the LWP reductions in the GCMs.

There is still considerable uncertainty over the processes which control turbulent cloud top entrainment, and so its treatment in turbulent mixing schemes in GCMs is necessarily incomplete. However, the GCMs lie on average in a regime where the MLM predicts that increases in turbulently driven entrainment will not reduce LWP substantially in the warmer climate, so this failing of the GCMs may not affect their cloud feedbacks substantially. Many of the CGILS SCMs do show evidence of enhanced entrainment of free tropospheric air into the boundary layer in the warmer climate however, but from entrainment which occurs through compensating subsidence when shallow convection penetrates the inversion. The MLM results highlight the potential impact of changes in entrainment on cloud feedback, clearly demonstrating its ability to change the sign of the LWP response. They also demonstrate that the sign of the response to the same large scale climate forcing can be positive or negative depending on the control state. This underscores the importance of testing the sensitivity to and improving the representation of entrainment processes, as well as reducing biases in the simulation of present-day subtropical clouds in GCMs. Additionally, most GCMs do not have sufficient vertical resolution to resolve the changes in cloud thickness and LWP predicted by the LES and MLM results. Coarse vertical resolution could result in GCMs responding to changes a drying of the boundary layer by reducing cloud fraction when they should maintain cloud fraction with a thinner cloud, distorting the cloud feedback response. Improved vertical resolution in the boundary layer would seem to be a necessary requirement for improved confidence in SCM and GCM cloud feedbacks.

WP4, entitled “Sensitivity experiments and hypothesis testing” has been responsible for developing and testing physical hypotheses relating to cloud feedback mechanisms, and testing them by performing sensitivity experiments with the GCMs. Initial work in WP4 reviewed sensitivity experiments based on parameter sensitivities. However, it was found that relationships that emerge from parameter-perturbed ensembles do not generalize to multi-model ensembles

A new conceptual framework for understanding cloud feedback mechanisms was developed, using the moist static energy (MSE) budget of the atmosphere. As the climate warms, changes in surface fluxes and clear-sky radiative cooling perturb the MSE budget of the atmosphere, creating an energetic imbalance which is balanced primarily by changes in cloudiness via longwave cloud cooling. In IPSL-CM5-LR (a model with one of the strongest cloud feedbacks) the low-level cloud feedback is related to the change in the vertical advection of low MSE air into the boundary layer from above, which strengthens in the warmer climate due to the Clausius-Clapeyron relation. The size of the cloud change is determined by the strength of the coupling between cloud properties and the longwave cloud radiative cooling, resulting in a relationship between the present day cloud fraction and the cloud feedback across different variants of IPSL-CM5-LR.

Applying the MSE budget framework to HadGEM2-A (a model with a weaker but still substantial positive feedback) showed that other terms in the MSE budget were more important in this case. Reductions in near-surface wind speed and air-sea temperature differences combined with increases in near-surface relative humidity were found to limit increases in surface evaporation and reduce sensible heat fluxes, inhibiting the turbulent transport of moisture from the surface to the cloud layer.

Examination of the surface fluxes in the CMIP5 GCMs shows reductions in sensible heat flux in the warmer climate, and relatively weak increases in surface latent heat flux in the more stable LTS regimes. These are due to reductions in air-sea temperature differences and near-surface wind speed, and increases in near-surface relative humidity, as found by previous studies. The relatively weak increases in surface evaporation could explain the tendency for models to show positive cloud feedbacks in stable subtropical regimes. Most of the GCMs show evidence of a deepening of the subtropical boundary layer with climate warming, which could well be a response enhanced entrainment of air into the boundary layer by shallow convection, as found in the CGILS SCMs.

The Selected Process On/Off Climate Intercomparison Experiment (SPOOKIE) is a recent initiative from WP4 which aims to establish the relative contributions of different areas of model physics to inter-model spread in cloud feedback by switching off or simplifying different model schemes in turn. Pilot experiments with parametrized convection switched off were found to exhibit a strong convergence in character compared to the standard model versions with parametrized convection, with the range in the global mean net cloud feedback being reduced by 43%. The net cloud feedback showed a reduced or similar spread across all tropical stability regimes, and a relatively smooth and monotonic transition from positive feedback in stable regimes to weakly negative feedback in unstable regimes. Much of the differing cloud fraction response (which is the dominant driver of cloud feedback spread across the low latitude oceans) is due to differences in parametrized convection in the participating models. Other features of the model response also show a considerable degree of convergence in the experiments, including changes in stability, subsidence, free tropospheric humidity and surface fluxes. These experiments indicate that differences in the parametrized convection responses in the models contribute substantially to inter-model spread in both deep convective and subtropical cloud feedbacks. Possible future experiments in which parametrized convection could be inhibited in deep convection regimes only would help to establish the extent to which these differences are due to remote controls of deep convection on subtropical cloud feedback, or the local influence of shallow convection. The presence of positive subtropical feedbacks in the absence of parametrized convection (albeit with reduced inter-model spread) does indicate however that processes other than shallow convective entrainment are contributing. The relatively weak increases in surface evaporation in the most stable regimes are still present without parametrized convection, and so remain as a potential candidate for explaining the general positive nature of subtropical cloud feedback. Another possibility is the Entrainment Liquid Flux (ELF) mechanism demonstrated in a recent LES study by Bretherton and Blossey (2014), where an increased cloud layer humidity flux in a warmer climate induces an entrainment liquid-flux adjustment that dries the stratocumulus cloud layer. Alternatively, the large scale component of the lower tropospheric mixing mechanism proposed by Sherwood et al. (2014) could be responsible. We plan to develop the SPOOKIE approach further in the future by

designing sensitivity tests for GCMs which target such remaining questions more directly.

The work of EUCLIPSE work packages 2,3 and 4 has provided many new insights into the mechanisms underlying the range of cloud feedbacks in contemporary climate models. As importantly, a number of new approaches have been developed and their utility demonstrated. Future investigations into cloud feedback mechanisms using the hierarchy of models, the MSE budget feedback analysis and sensitivity experiment based hypothesis testing frameworks developed in EUCLIPSE will continue and will undoubtedly yield further insights in the future.

## **Acknowledgements**

We are grateful to Adrian Lock, Thorsten Mauritsen, Masahiro Watanabe, Tsuyoshi Koshiro and Hideaki Kawai useful discussions and for contributing model data for the SPOOKIE intercomparison presented in this report.

## **Bibliography**

Studies with EUCLIPSE supported authors are marked with \*.

\*Andrews, T., J. M. Gregory, M. J. Webb, and K. E. Taylor (2012), Forcing, feedbacks and climate sensitivity in CMIP5 coupled atmosphere-ocean climate models, *Geophys. Res. Lett.*, **39**, L09712, doi:10.1029/2012GL051607.

\*Blossey, P. N., Bretherton, C. S., Zhang, M. and co-authors. (2013): Marine low cloud sensitivity to an idealized climate change: The CGILS LES intercomparison. *Journal of Advances in Modeling Earth Systems*, **5**, 234–258, doi:10.1002/jame.20025.

Bony, S. and Dufresne, J. L. (2005). Marine boundary layer clouds at the heart of tropical cloud feedback uncertainties in climate models. *Geophysical Research Letters*, **32**, doi: 10.1029/2005GL023851

Bony, S., and co-authors. (2011), CFMIP: Towards a better evaluation and understanding of clouds and cloud feedbacks in CMIP5 models. *Clivar Exchanges*, **56**, 16, 2.

Bretherton, C. S., Blossey, P. N., and Jones, C. R. (2013): Mechanisms of marine low cloud sensitivity to idealized climate perturbations: A single LES exploration extending the CGILS cases. *Journal of Advances in Modeling Earth Systems*, **5**, 316–337, doi:10.1002/jame.20019.

Bretherton, C. S., and Blossey, P. N. (2014): Low cloud reduction in a greenhouse-warmed climate: Results from Lagrangian LES of a subtropical marine cloudiness transition. *J. Adv. Model. Earth Syst.*, doi:10.1002/2013MS000250.

Chikira, M. and Sugiyama, M. (2010). A cumulus parameterization with state-dependent entrainment rate. Part I: Description and sensitivity to temperature and humidity profiles. *Journal of the Atmospheric Sciences*, **67**, 2171-2193.

\*Dal Gesso, S., A. P. Siebesma, S. R. de Roode, and J. M. van Wessem, 2013: A mixed-layer model perspective on stratocumulus steady-states in a perturbed climate. *Q. J. R. Meteor. Soc.*, in press.

\*Dal Gesso, S., A. P. Siebesma, and S. R. de Roode, 2013: Evaluation of low-cloud climate feedback through Single-Column Model equilibrium states. Submitted to the *Q. J. R. Met. Soc.*

\*de Roode, S.R., A. P. Siebesma, S. Dal Gesso, H. J. J. Jonker, J. Schalkwijk, and J. Sival, (2012): The stratocumulus response to a single perturbation in cloud controlling factors. Submitted to *J. Climate*.

Gregory, J. M., Ingram, W. J., Palmer, M. A., Jones, G. S., Stott, P. A., Thorpe, R. B., and co-authors (2004). A new method for diagnosing radiative forcing and climate sensitivity. *Geophysical Research Letters*, **31**, L03205, doi:10.1029/2003GL018747.

Gregory, J.M. and M.J. Webb (2008), Tropospheric adjustment induces a cloud component in CO<sub>2</sub> forcing. *J. Climate*, **21**, 58-71, doi :10.1175/2007JCLI1834.1.

\*Klocke, D., Pincus, R., and Quaas, J. (2011): On constraining estimates of climate sensitivity with present-day observations through model weighting. *Journal of Climate*, **24**, 6092-6099.

Richter, I., and Xie, S. P. (2008): Muted precipitation increase in global warming simulations: A surface evaporation perspective. *Journal of Geophysical Research: Atmospheres*, **113**, D24118, doi:10.1029/2008JD010561.

\*Rieck, M., Nuijens, L., and Stevens, B. (2012): Marine boundary layer cloud feedbacks in a constant relative humidity atmosphere. *Journal of the Atmospheric Sciences*, **69**, 2538-2550.

\*Sherwood, S.C., Bony, S. and Dufresne, J.-L. (2014) Spread in model climate sensitivity traced to atmospheric convective mixing. *Nature*, **505**, 37–42, doi:10.1038/nature12829

Siebesma, A. P., Jakob, C., Lenderink, G. and co-authors. (2004). Cloud representation in general circulation models over the northern Pacific Ocean: A EUROCS intercomparison study. *Quarterly Journal of the Royal Meteorological Society*, **130**, 3245-3267.

Soden, B. J., Held, I. M. and coauthors. (2008). Quantifying climate feedbacks using radiative kernels. *Journal of Climate*, 21(14), 3504-3520.

Taylor, K.E., R.J. Stouffer and G.A. Meehl (2011), An overview of CMIP5 and the experiment design. *Bull. Amer. Meteor. Soc.*, doi:10.1175/BAMS-D-11-00094.1.

Teixeira, J. and co-authors. (2011), Tropical and Subtropical Cloud Transitions in Weather and Climate Prediction Models: The GCSS/WGNE Pacific Cross-Section Intercomparison (GPCI). *J. Climate*, **24**, 5223–5256. doi: <http://dx.doi.org/10.1175/2011JCLI3672.1>

\*Vial, J., Dufresne, J. L., and Bony, S. (2013): On the interpretation of inter-model spread in CMIP5 climate sensitivity estimates. *Climate Dynamics*, **41**, 3339–3362, DOI 10.1007/s00382-013-1725-9.

Webb, M. J., Senior, C. A., Sexton, D. M. H., Ingram, W. J., Williams, K. D., Ringer, M. A. and co-authors. On the contribution of local feedback mechanisms to the range of climate sensitivity in two GCM ensembles. *Climate Dynamics*, **27**, 17-38.

\*Webb, M. J., Lambert, F. H. and Gregory, J. M. Origins of differences in climate sensitivity, forcing and feedback in climate models (2013): *Climate Dynamics*, **40**, 677-707.

\*Webb, M.J. and Lock, A.P. (2013): Coupling between subtropical cloud feedback and the local hydrological cycle in a climate model. *Climate Dynamics*, **41**, 1923-1939.

\*Webb, M. J., Lock, A.P., Bodas-Salcedo, A., Bony, S., Cole, J.N.S., Koshiro, T., Kawai, H., Lacagnina, C., Selten, F., Roehrig, R., Stevens, B. The diurnal cycle of

cloud feedback and land surface warming in climate models. Submitted to *Climate Dynamics*.

Zhang M., C. S. Bretherton, (2008) Mechanisms of low cloud climate feedback in idealized single-column simulations with the community atmospheric model (CAM3). *J. Climate*, **21**,4859–4878. doi:10.1175/2008JCLI2237.1

\*M. Zhang, C. S. Bretherton, P. N. Blossey, S. Bony, F. Brient and J.-C. Golaz, (2012): The CGILS Experimental Design to Investigate Low Cloud Feedbacks in General Circulation Models by Using Single-Column and Large-Eddy Simulation Models. In press, *J. Adv. Model. Earth Syst.*, doi:10.1029/2012MS000182

\*Zhang, M. and co-authors. (2013): CGILS: Results from the first phase of an international project to understand the physical mechanisms of low cloud feedbacks in single column models. *Journal of Advances in Modeling Earth Systems*. doi: 10.1002/2013MS000246.

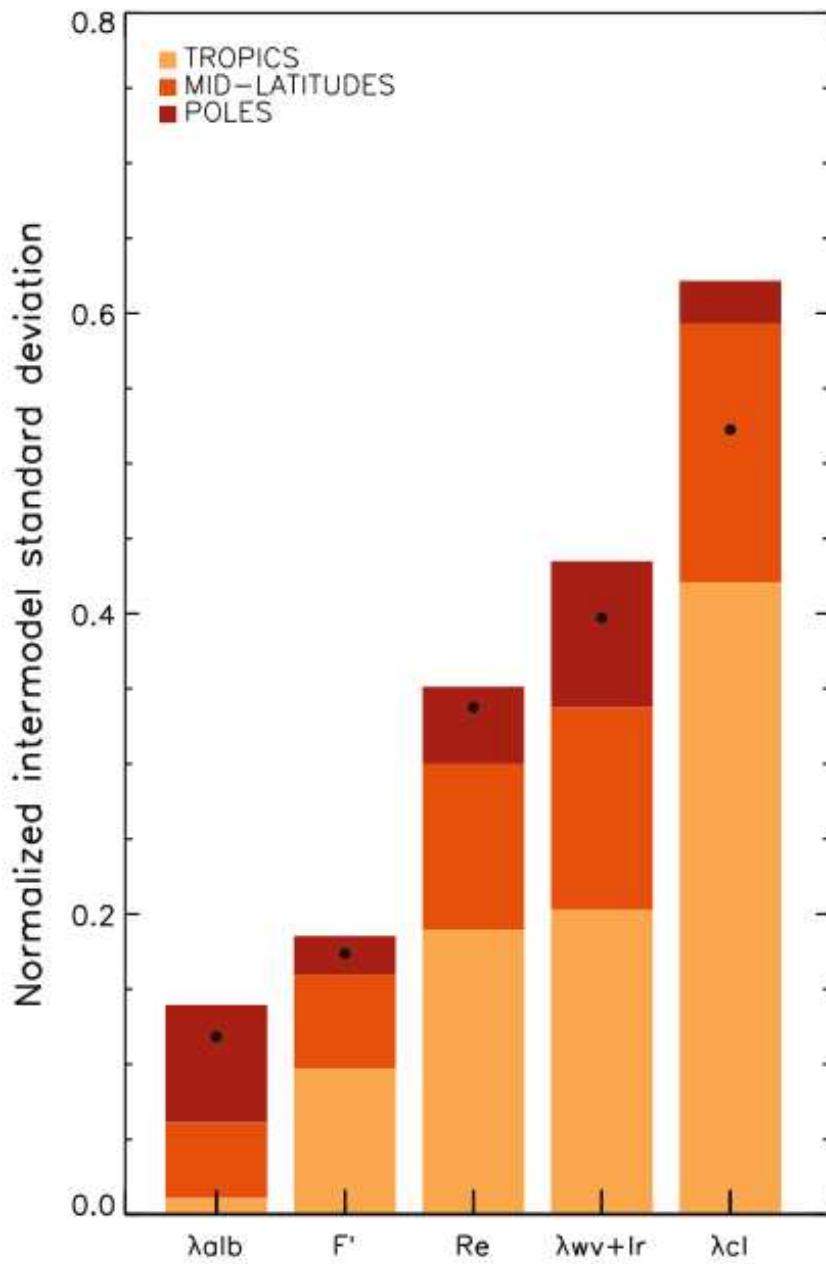


**Figure 1.** Decomposition of CMIP5 climate sensitivity spread (normalised standard deviation) into contributions from  $\lambda_{alb}$  (surface albedo feedback),  $F'$  ( $CO_2$  forcing),  $Re$  (kernel residual term),  $\lambda_{wv} + \lambda_{lr}$  (water vapour plus lapse rate feedback) and  $\lambda_{cl}$  (cloud feedback). From Vial et al. (2013).

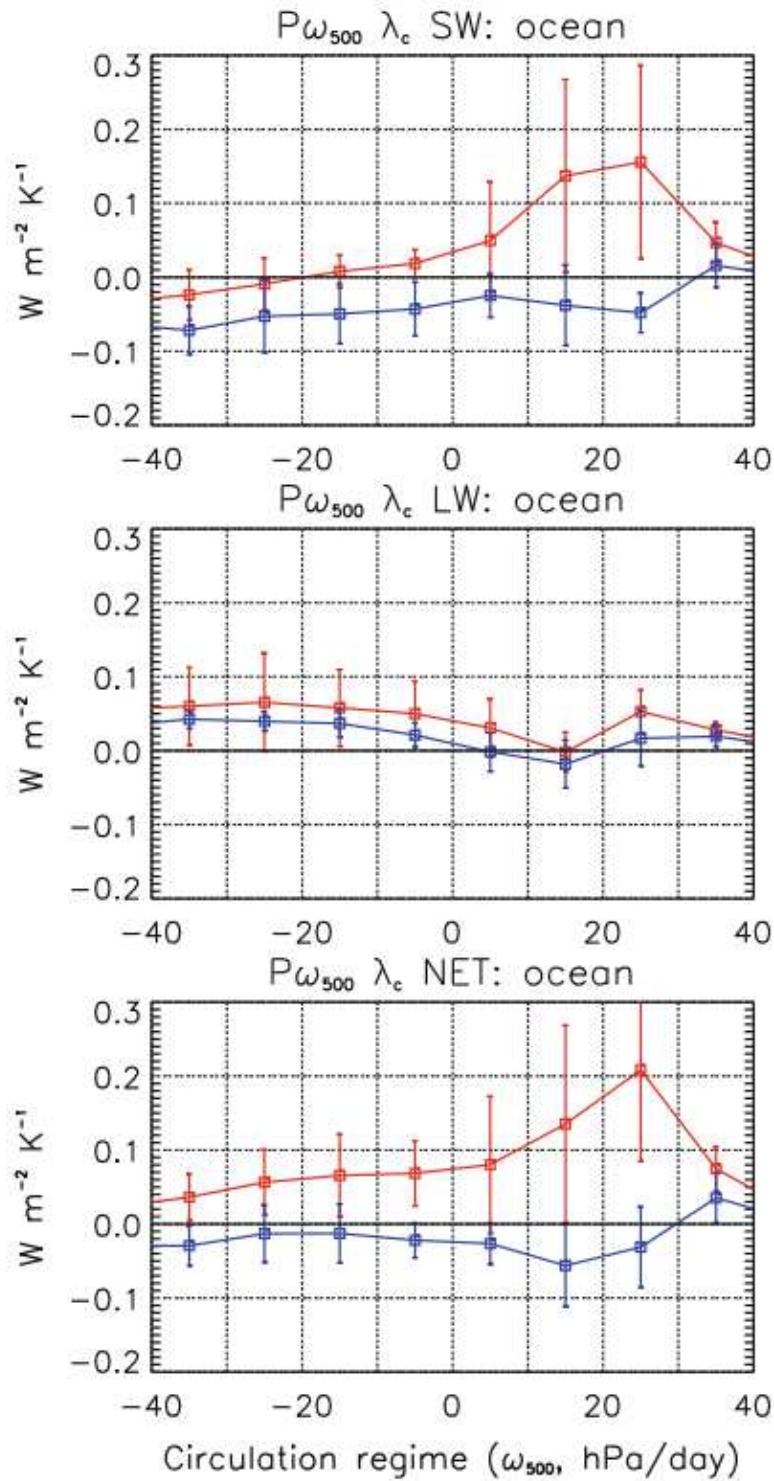


**Figure 2.** Inter-model spread in shortwave, longwave and net cloud feedback within 500mb pressure velocity circulation regimes in the tropics (Vial et al. 2013). The red lines show thermodynamic components of the feedbacks, averaged over all cases which fall into the regime, and across the 50% most sensitive climate models. The blue lines show the equivalent for the lower 50%, and vertical bars show the standard deviations across models within each group.

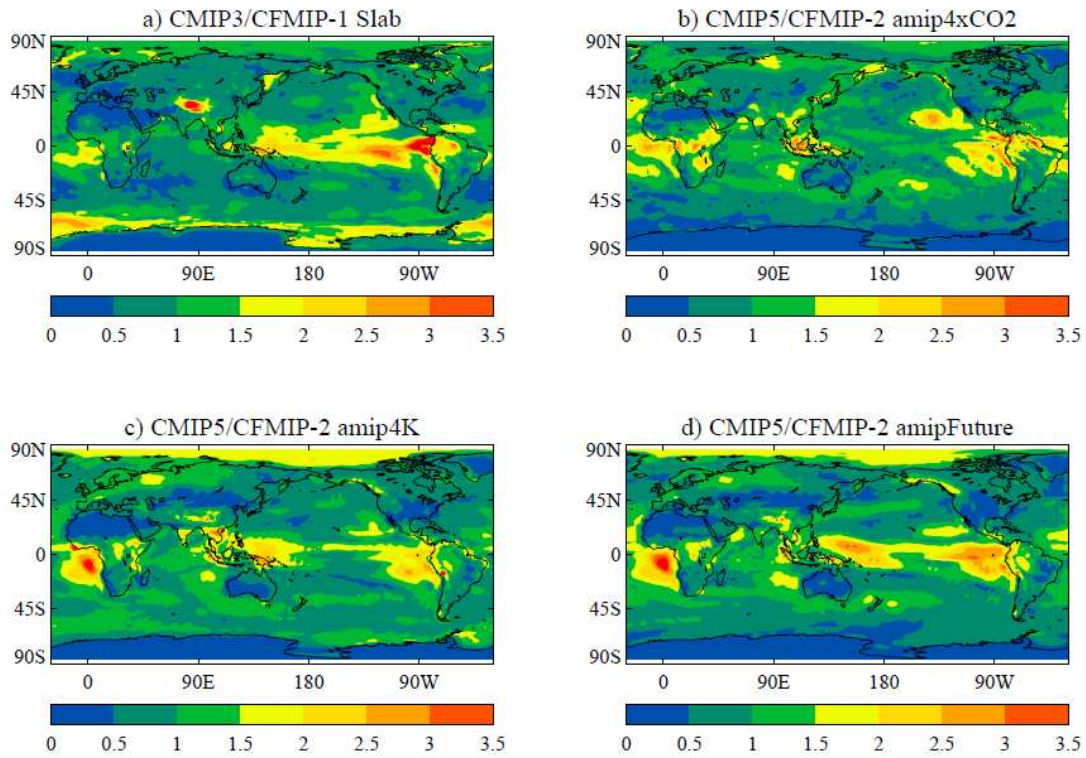


**Figure 3.** Relative contributions of different parts of the globe to inter-model spread in cloud feedbacks (a,c and d) and cloud adjustments (b). The maps show local standard deviations across each ensemble, normalised to have global means equal to unity to support a visual comparison of the regions responsible for the largest inter-model spread.

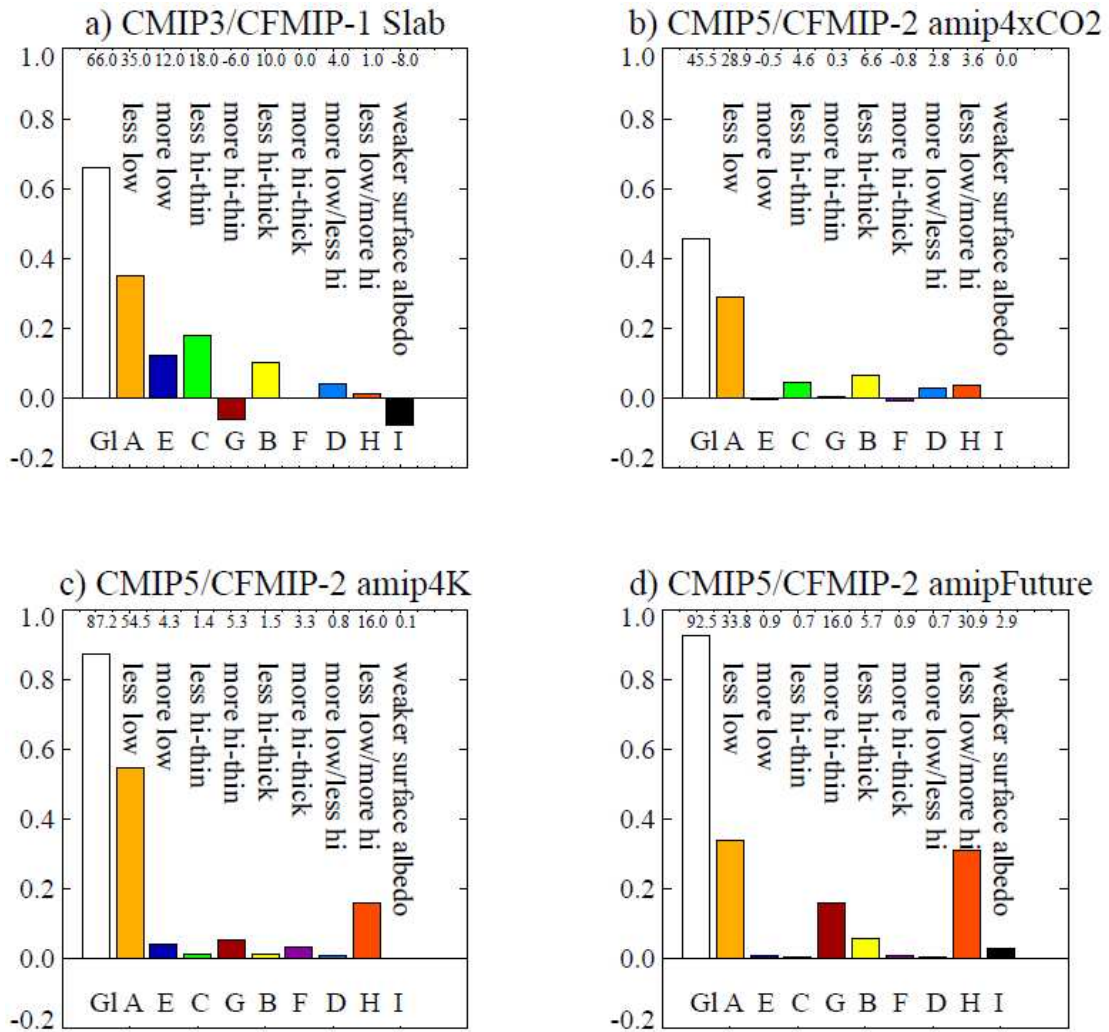


**Figure 4: Contributions to inter-model spread in cloud feedbacks (a,c,d) and cloud adjustments (b) from the cloud feedback classes from Webb et al. (2006).** The white bars show the percentage of the variance in the total feedback and adjusted forcing across each ensemble due to global cloud feedback or adjustment. The coloured bars show the contributions from the individual feedback classes.

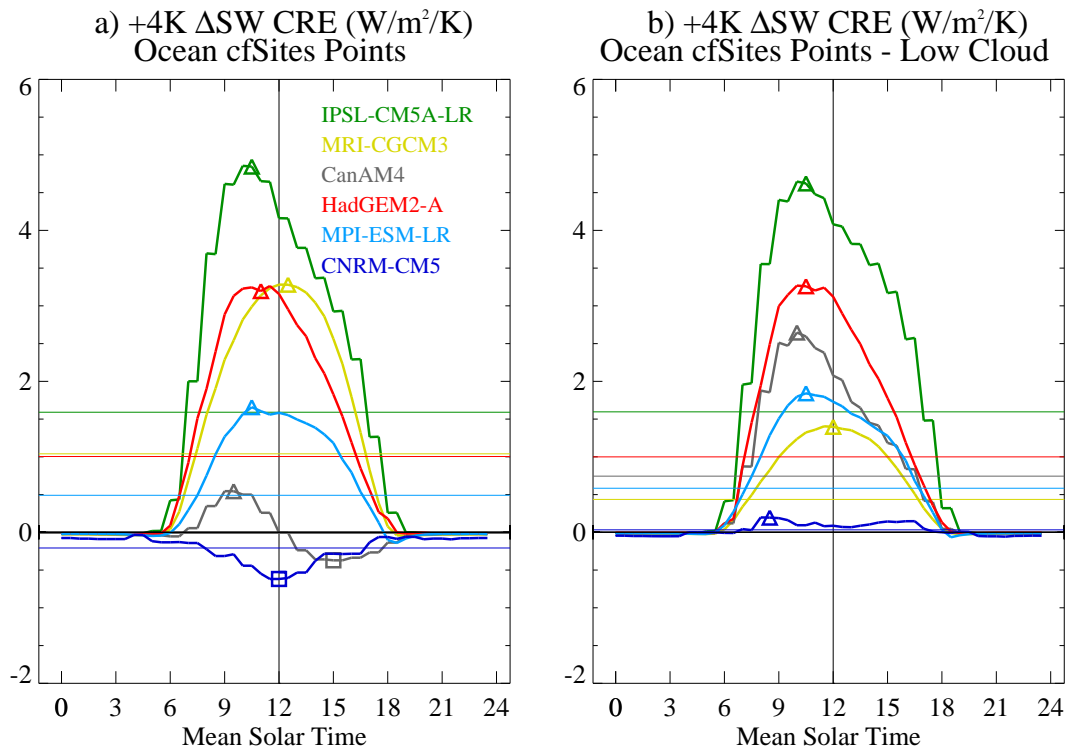


**Figure 5.** Diurnal cycle of the Shortwave Cloud Radiative Effect (CRE) averaged over cfSites ocean locations in AMIP and uniform +4K perturbation experiments. a) shows diurnally resolved shortwave CRE responses to the uniform +4K SST perturbation, normalised by the global mean near-surface temperature response. b) shows the contributions to these from occasions when the low clouds are dominant. From Webb et al. (submitted).

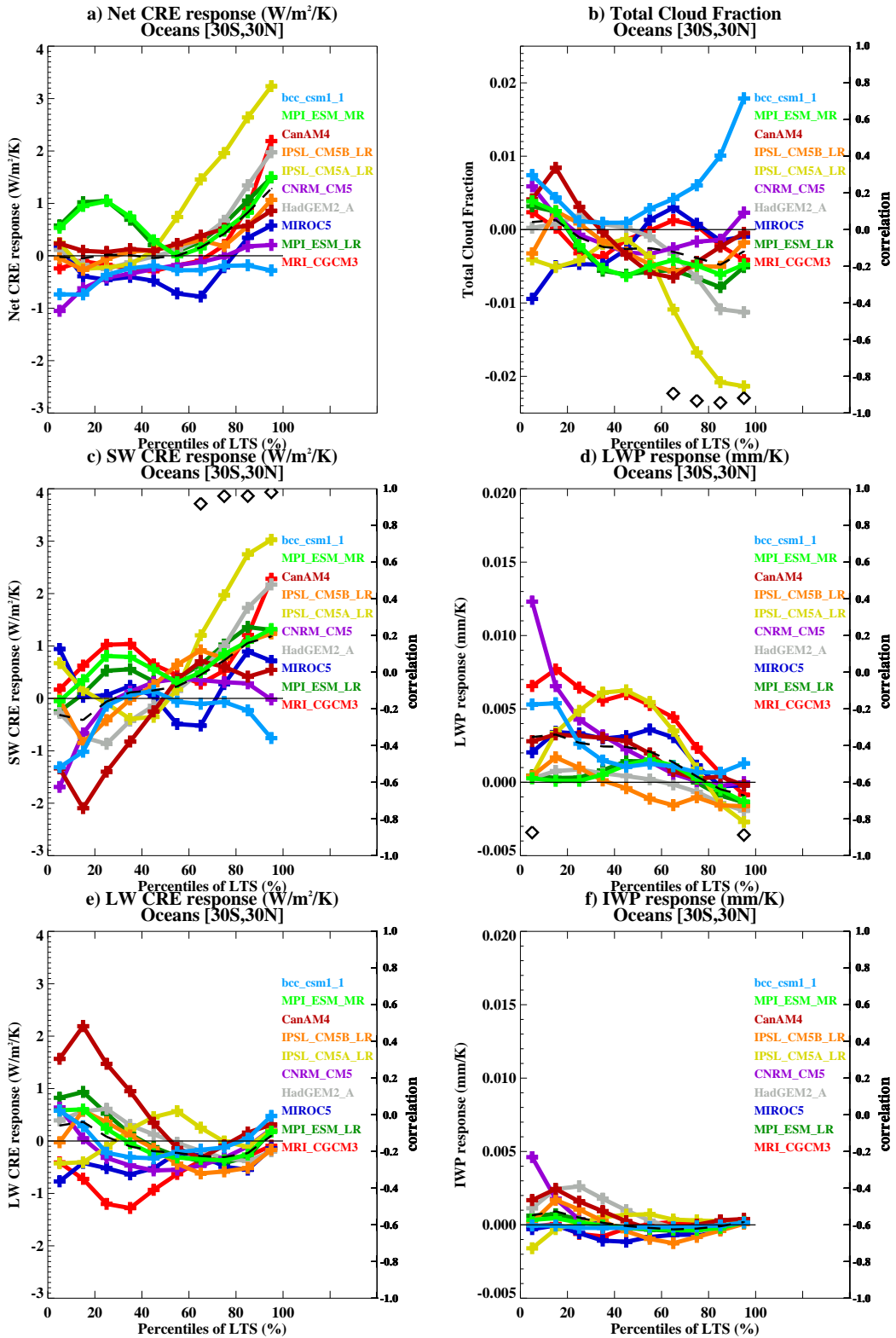


**Figure 6.** LTS composites of net, shortwave and longwave cloud feedback over low latitude oceans (30N/S) in the amip4K experiments. Also shown are responses of total cloud fraction, liquid water path and ice water path, expressed per degree of global near surface temperature change. The dashed black lines shows the ensemble mean responses. Diamonds indicate a correlation with the net CRE response which is greater than 0.8.

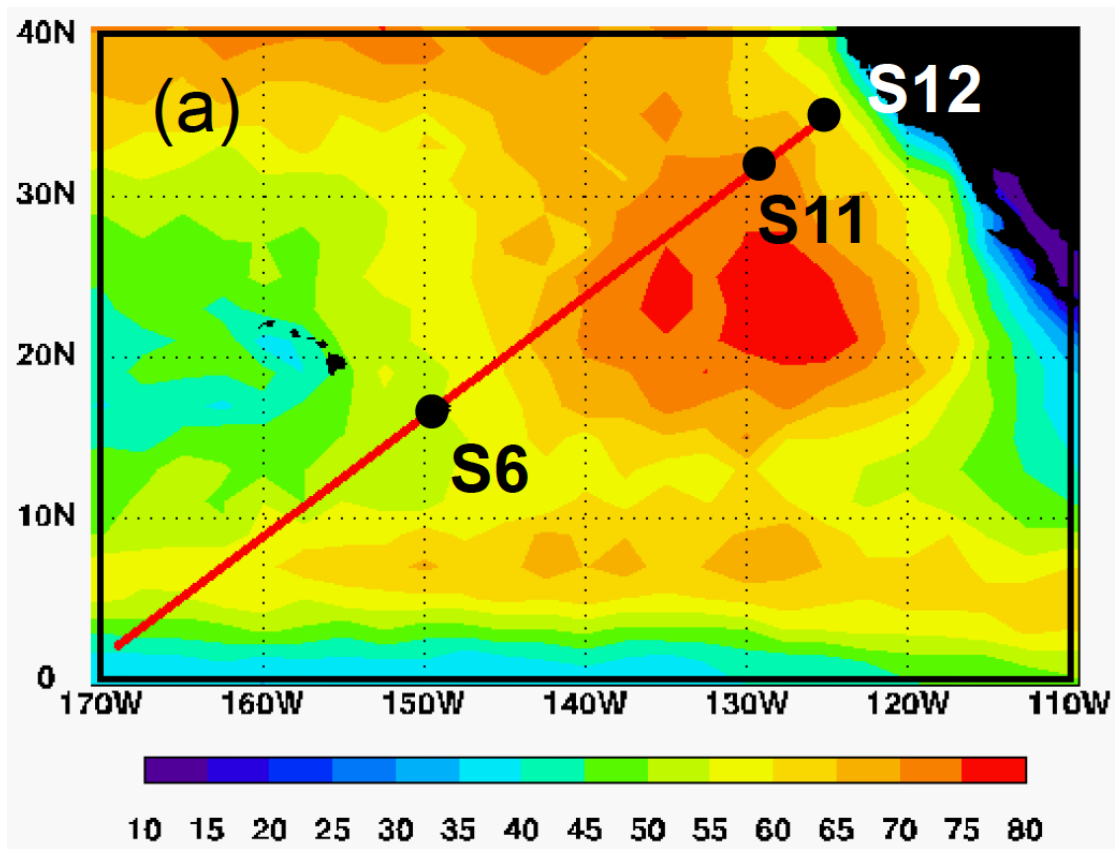


**Figure 7.** Averaged amount of low clouds in June-July-August (%). The red line is the northern portion of the GPCI. The symbols 'S6', 'S11' and 'S12' are the three locations used in the CGILS experiments (From Zhang et al., 2012a).

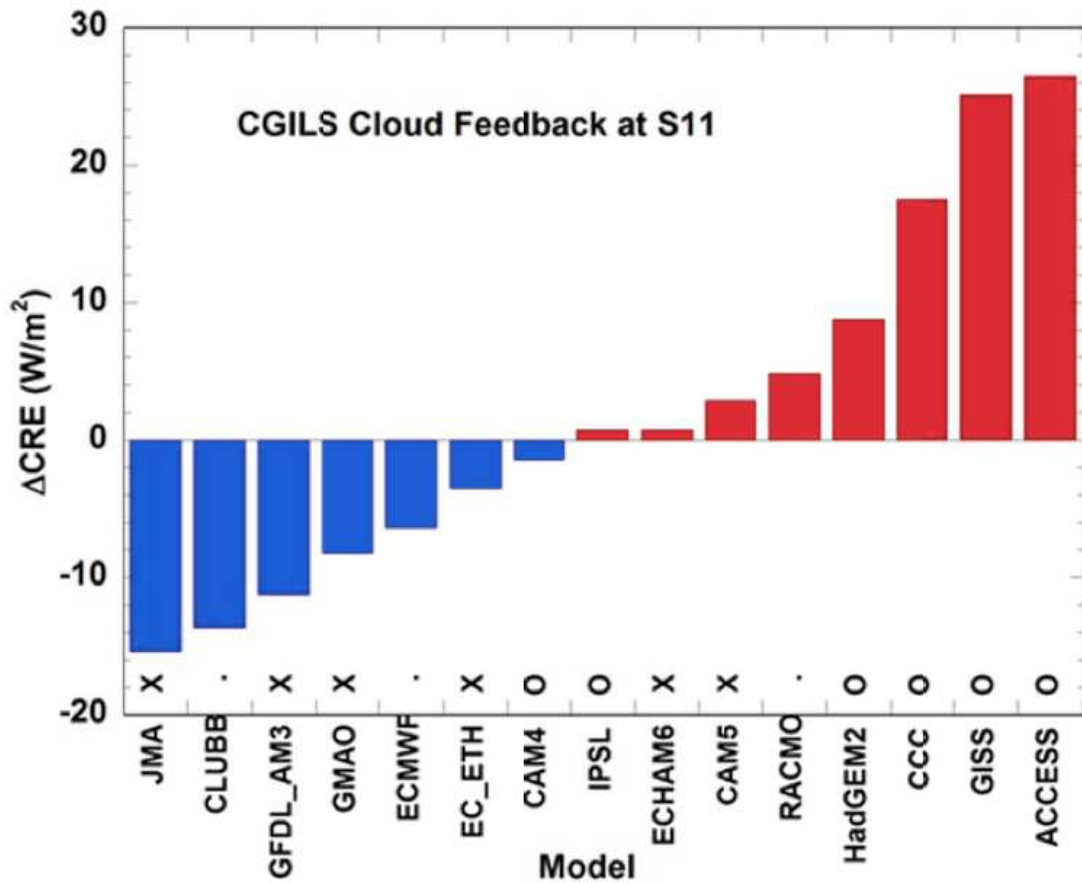


**Figure 8.** Change of cloud radiative effect (CRE, W/m<sup>2</sup>) in SCMs at location S11 in response to a 2K SST perturbation. An “X” above a model’s name indicates that the shallow convection scheme is not active; “O” indicates that the shallow convection scheme is active. Models without these characters either do not separately parameterize shallow convection and PBL turbulence, or did not submit results with convection information. From Zhang et al. (2013).

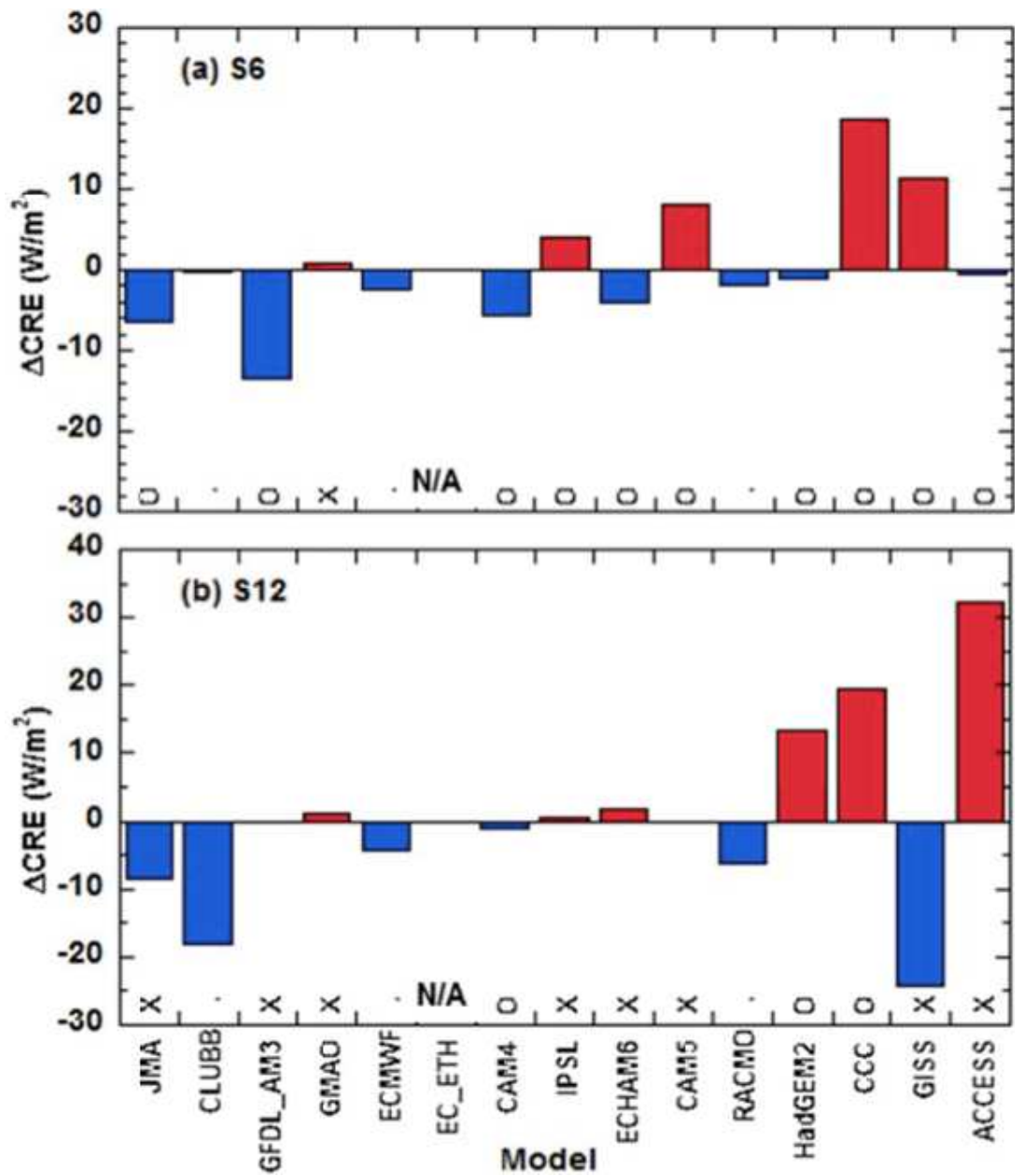


**Figure 9.** Same as Figure 8, but for (a) S6, (b) S12. The models in the same order as in Figure 8. One model (EC\_ECH) did not reach quasi-equilibrium state and it is indicated by “N/A”. From Zhang et al. (2013).

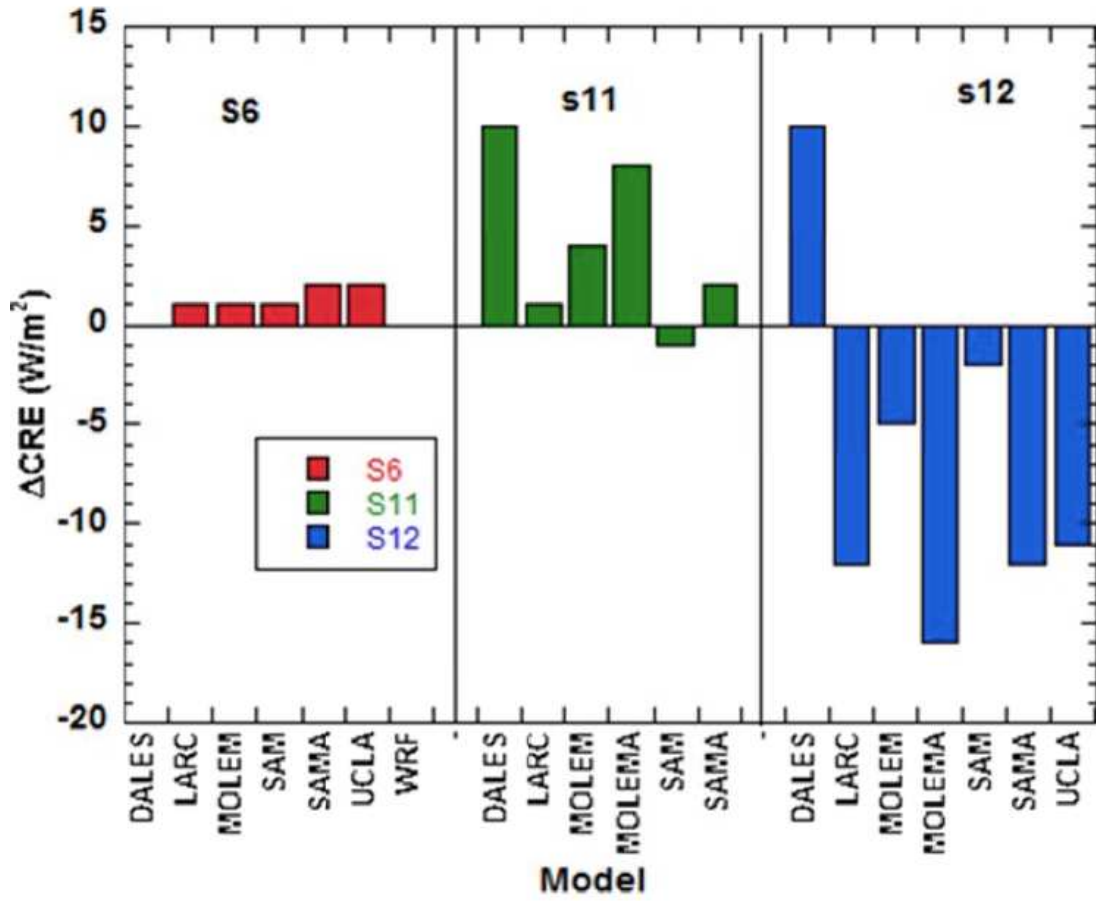


**Figure 10.** Same as Figures 8 and 9 but for the LES models. From Zhang et al. (2013).

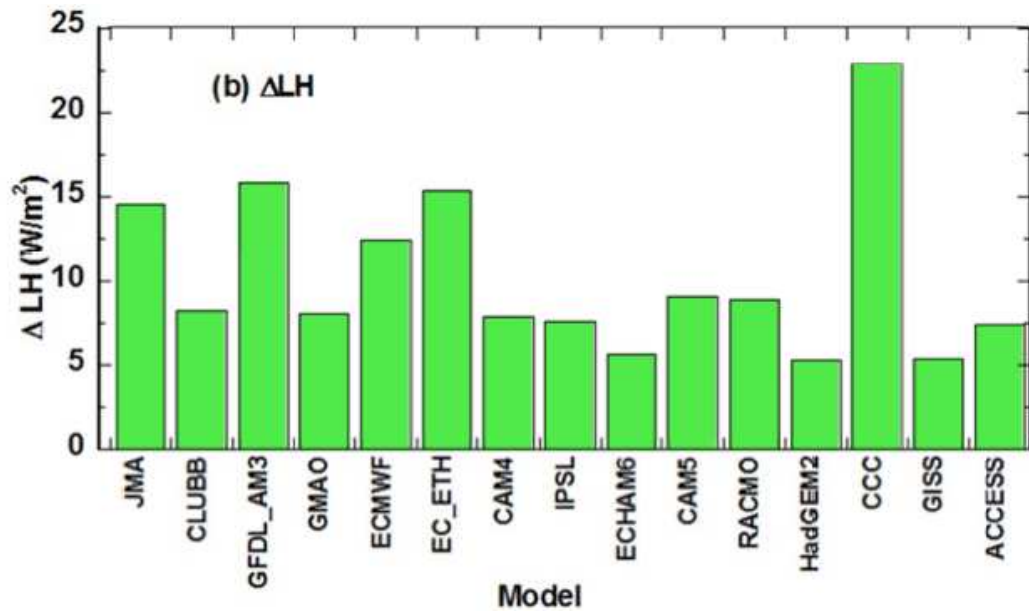


**Figure 11.** Change of surface latent heat flux in the SCMs from the control climate to the perturbed climate at S11 ( $W/m^2$ ). From Zhang et al. (2013).

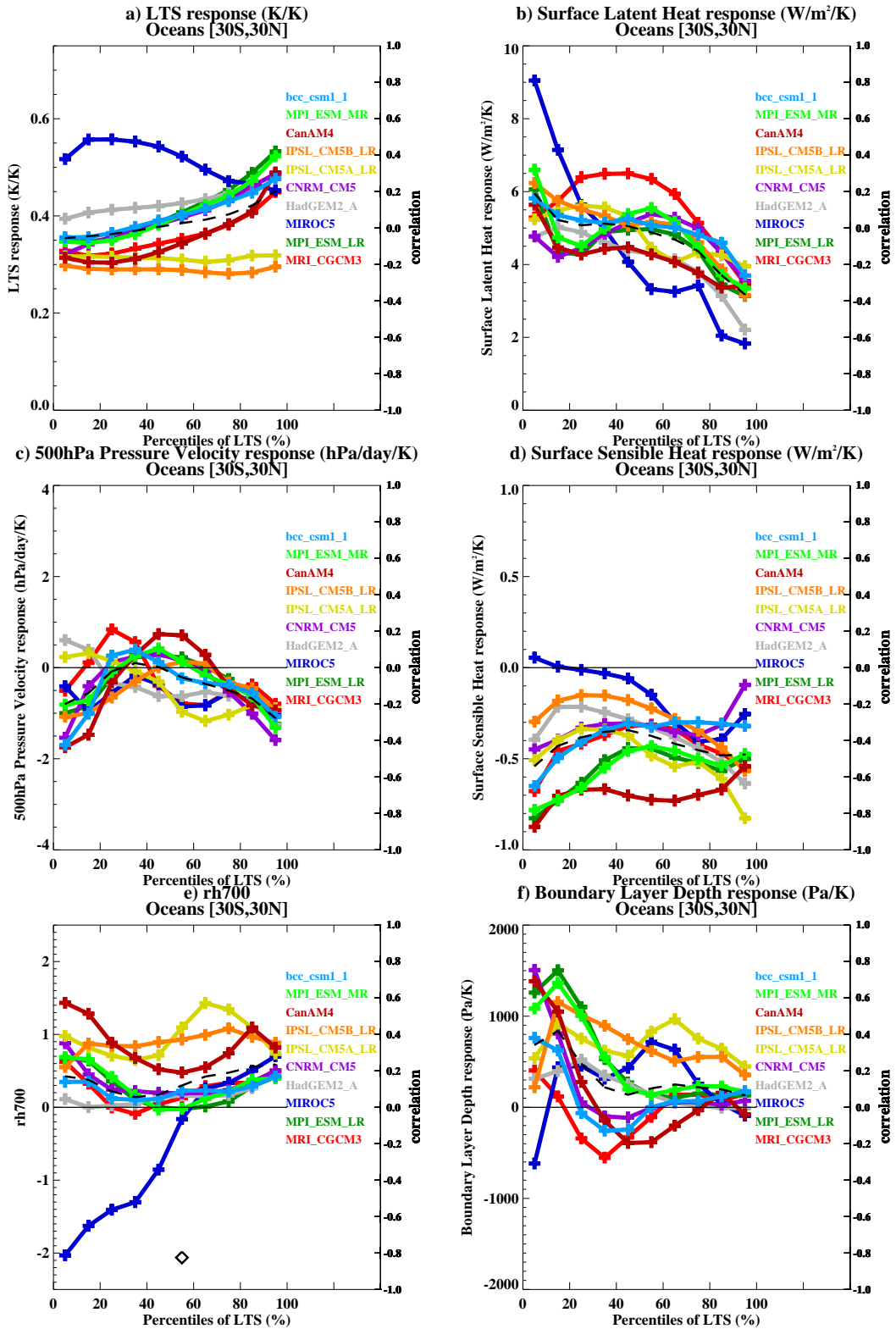


**Figure 12.** As Figure 6 but for responses of LTS, 500mb Vertical Pressure Velocity, Precipitation, Surface Latent and Sensible Heat fluxes, and Boundary Layer Depth defined as the difference between the surface pressure and the pressure level at which relative humidity drops below 50 percent.

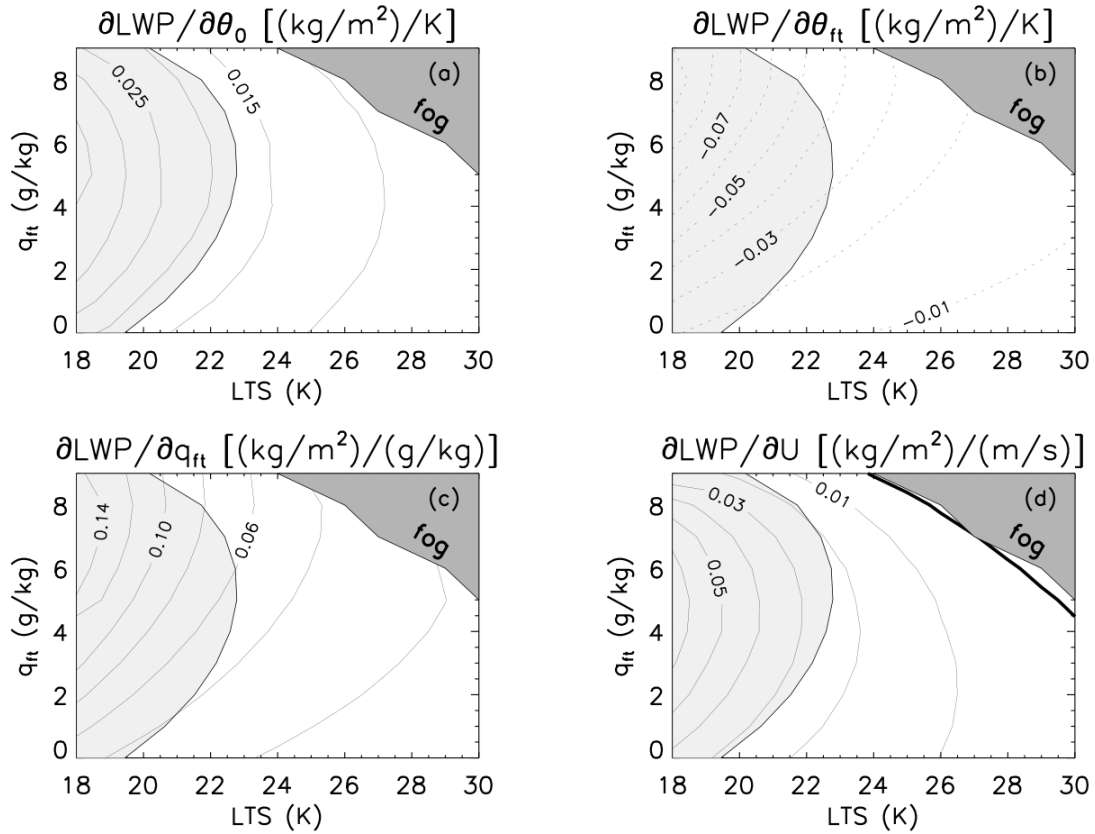


**Figure 13.** The total response of the liquid water path with fixed cloud top entrainment to changes in (a) the potential sea surface temperature  $\theta_0$ , (b) the free tropospheric potential temperature  $\theta_{ft}$ , (c) the free tropospheric specific humidity  $q_{ft}$  and (d) the horizontal wind speed  $U$ . The thick solid line indicates the zero isoline. The dark grey shaded area depicts fog situations in which the cloud-base height is at the sea surface, and the light grey shaded area represents boundary layers that are warmer than the sea surface.

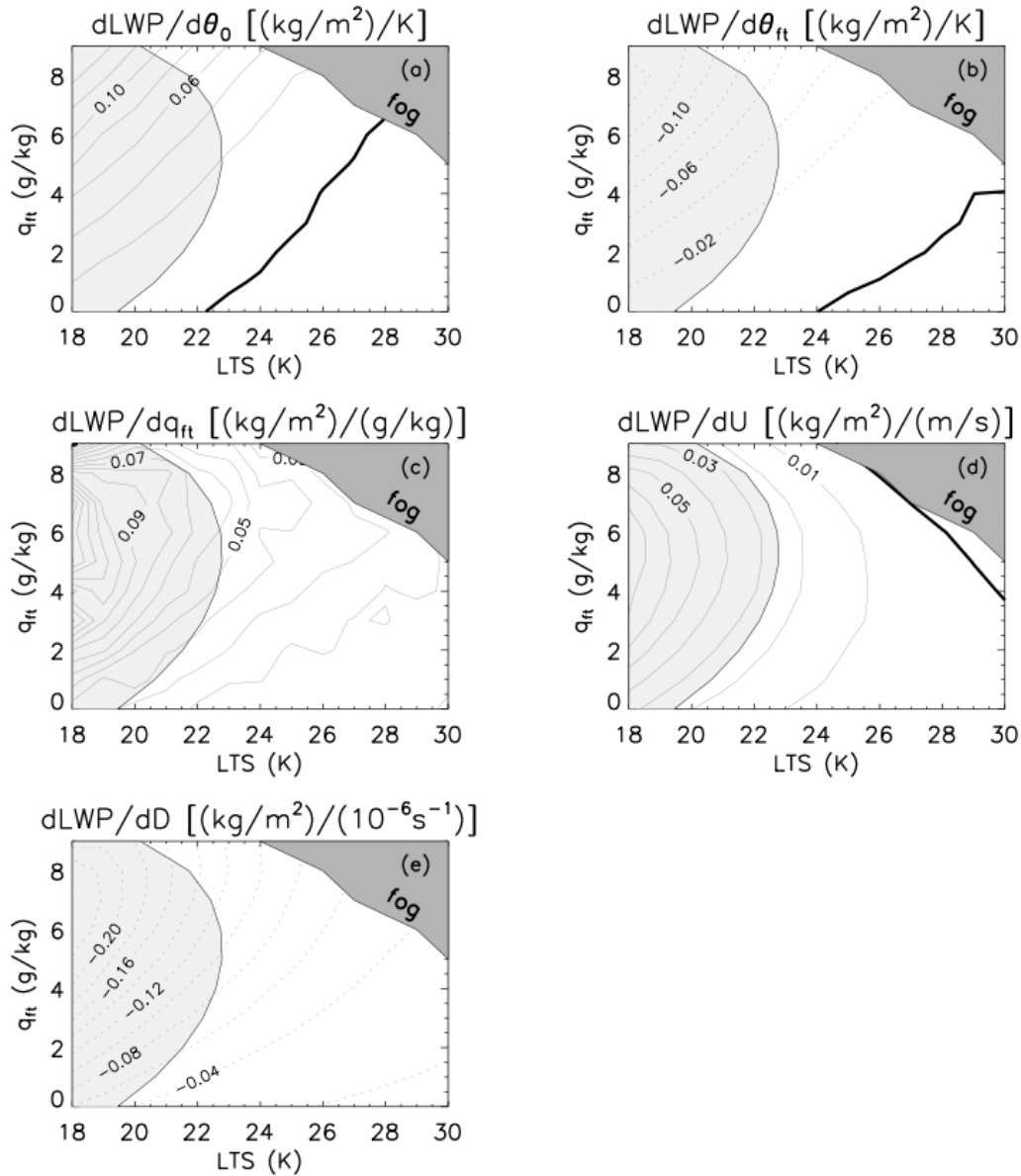


**Figure 14.** The total response of the liquid water path with interactive cloud top entrainment to changes in (a) the potential sea surface temperature  $\theta_0$ , (b) the free tropospheric potential temperature  $\theta_{ft}$ , (c) the free tropospheric specific humidity  $q_{ft}$ , (d) the horizontal wind speed  $U$  and (e) the large-scale divergence  $D$ . The thick solid line indicates the zero isoline. The dark grey shaded area depicts fog situations in which the cloud-base height is at the sea surface, and the light grey shaded area represents boundary layers that are warmer than the sea surface.

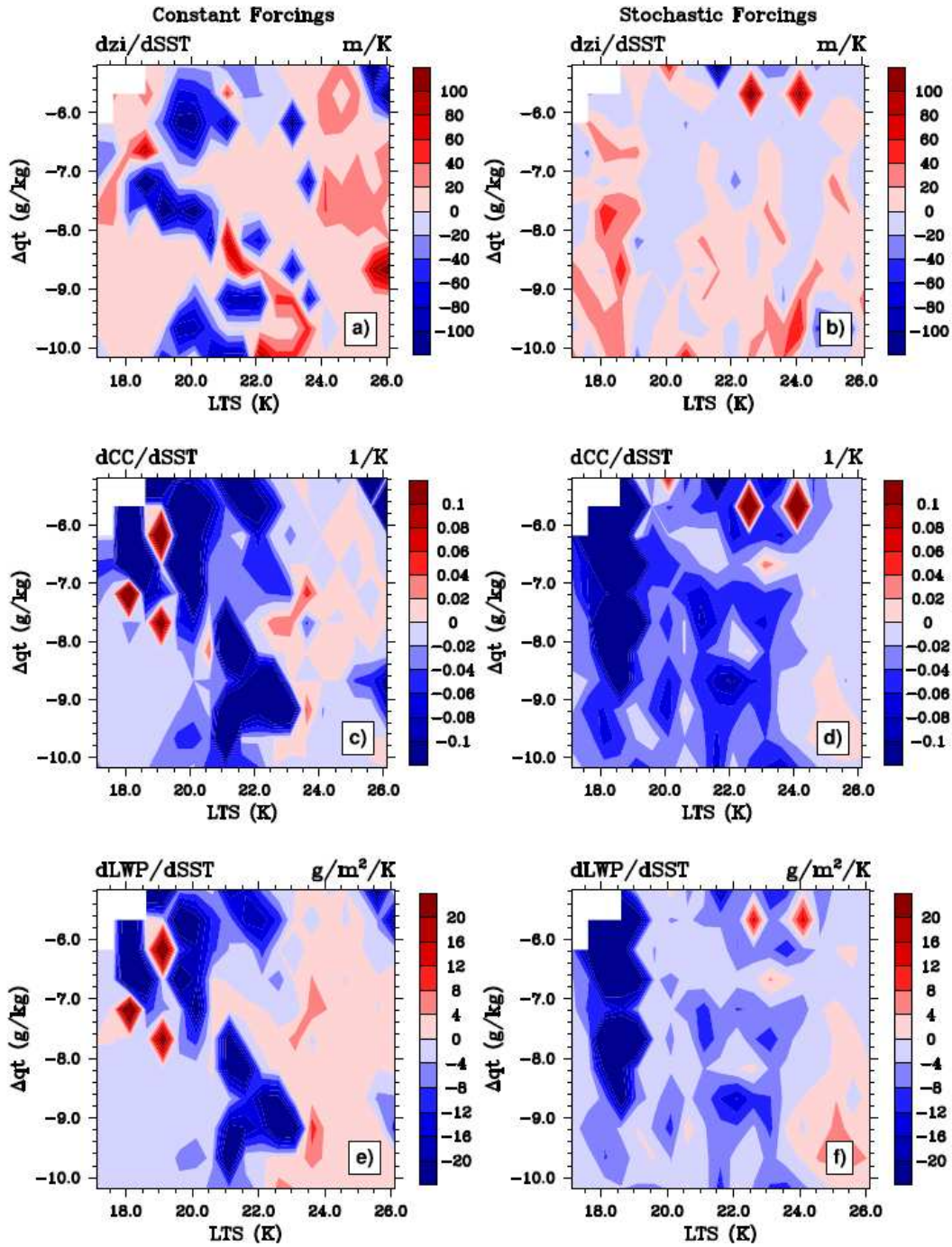


Figure 15. Phase space results of changes in the inversion height  $z_i$ , cloud cover CC and LWP to a climate perturbation for constant (left column) and stochastic forcings (right column) experiments with the KNMI EC-EARTH SCM. The white area corresponds to the free tropospheric conditions for which the deep convection scheme is active.

### HadGem2

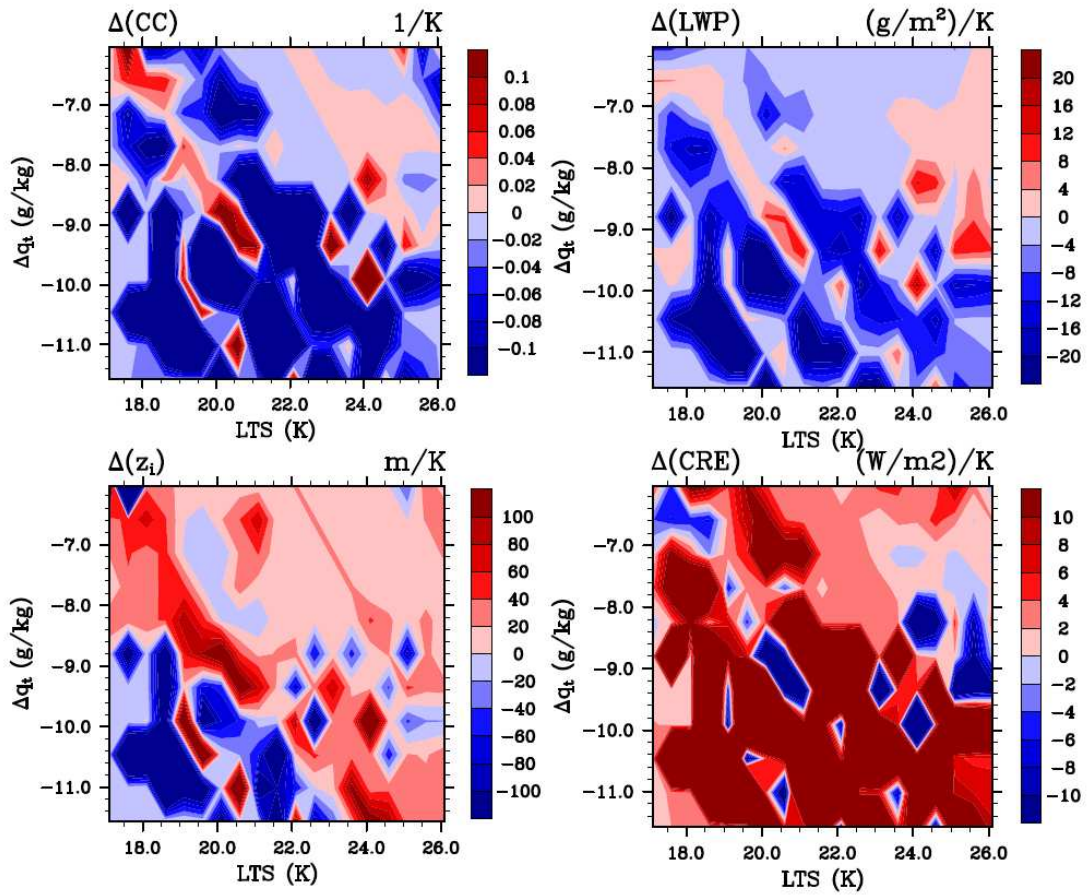
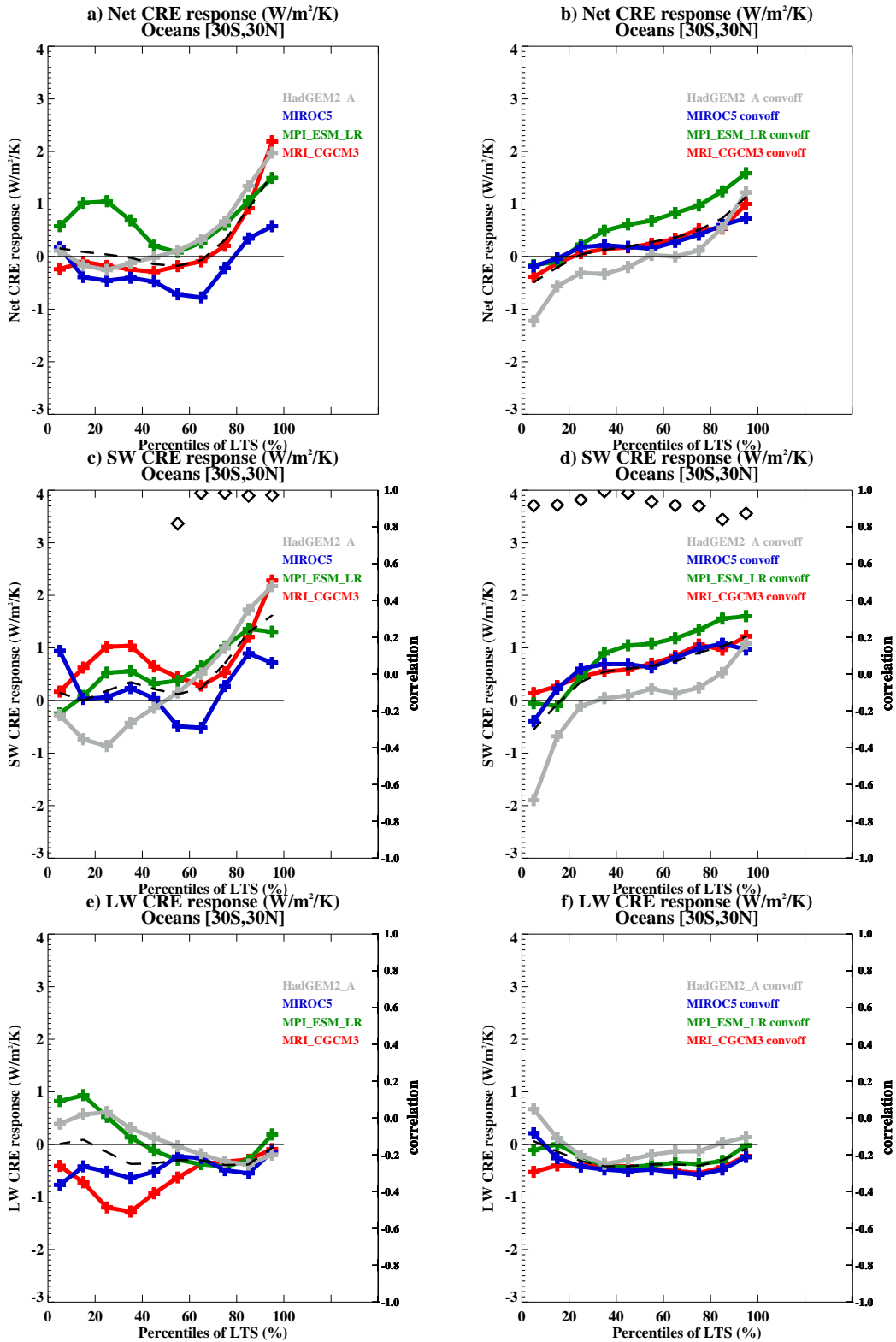
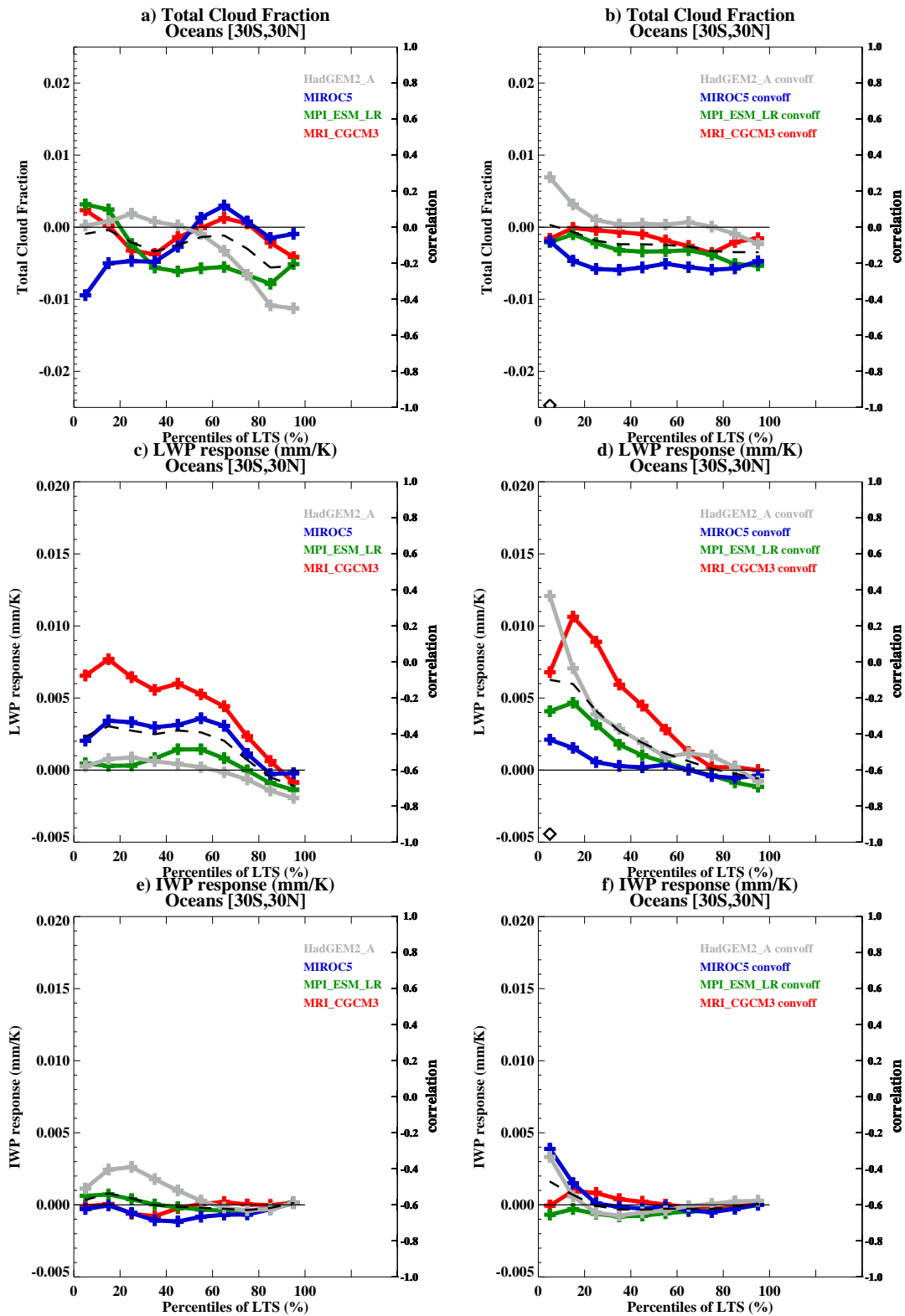


Figure 16. Phase space results of changes in the cloud cover CC , LWP, inversion height  $z_i$ , and Cloud Radiative Effect (CRE) to a climate perturbation with the UKMO SCM.



**Figure 17.** LTS composites of net, shortwave and longwave cloud feedback over low latitude oceans (30N/S) in the amip/amip4K experiments (left) and convoffamip/convoffamip4K SPOOKIE experiments without parametrized convection (right). The dashed black lines shows the ensemble mean responses. Diamonds indicate a correlation with the net CRE response which is greater than 0.8.



**Figure 18.** As Figure 17 but for total cloud fraction, LWP and IWP responses.

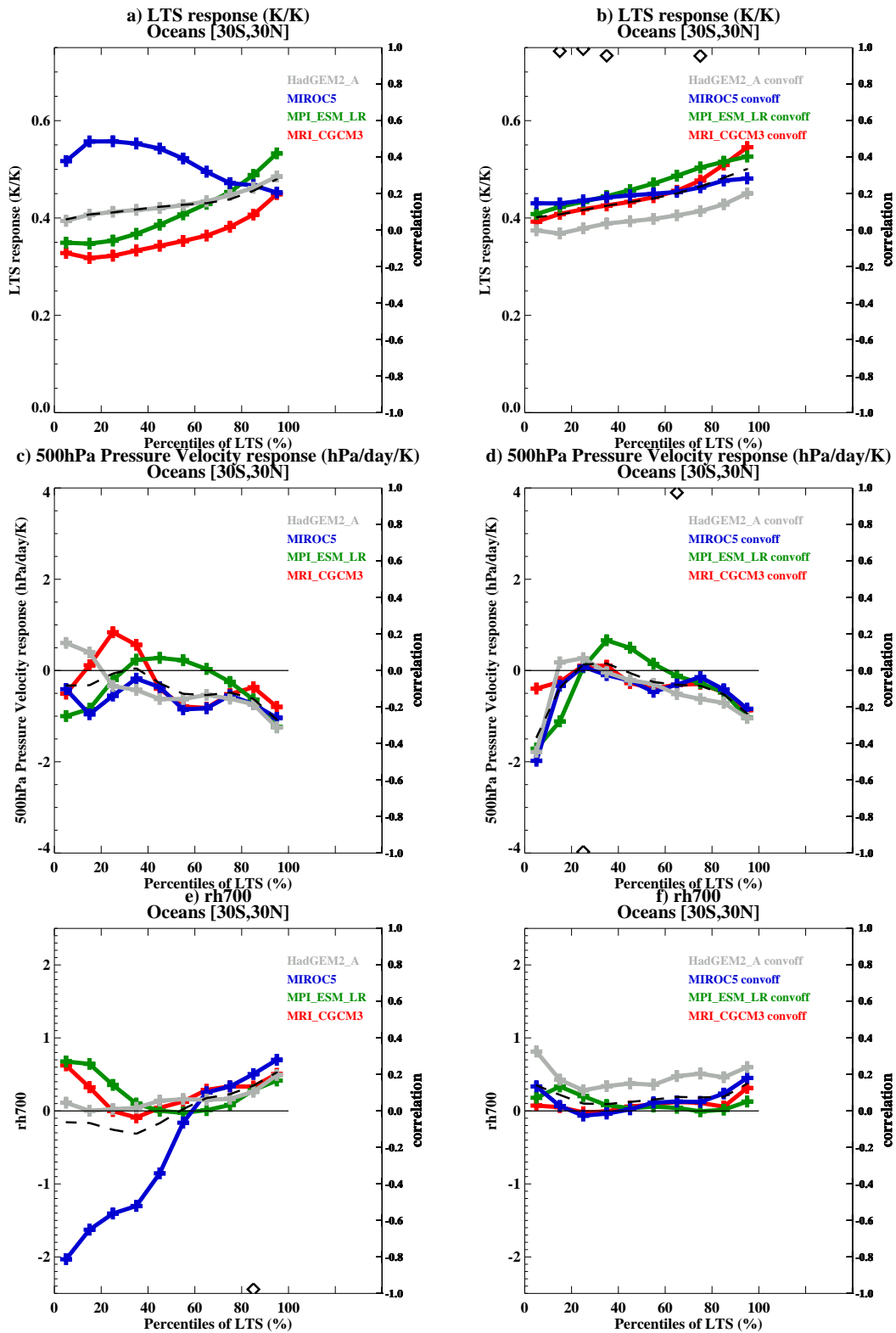


**Figure 19.** As Figure 17 but for LTS, 500hPa pressure velocity and 700hPa relative humidity responses.

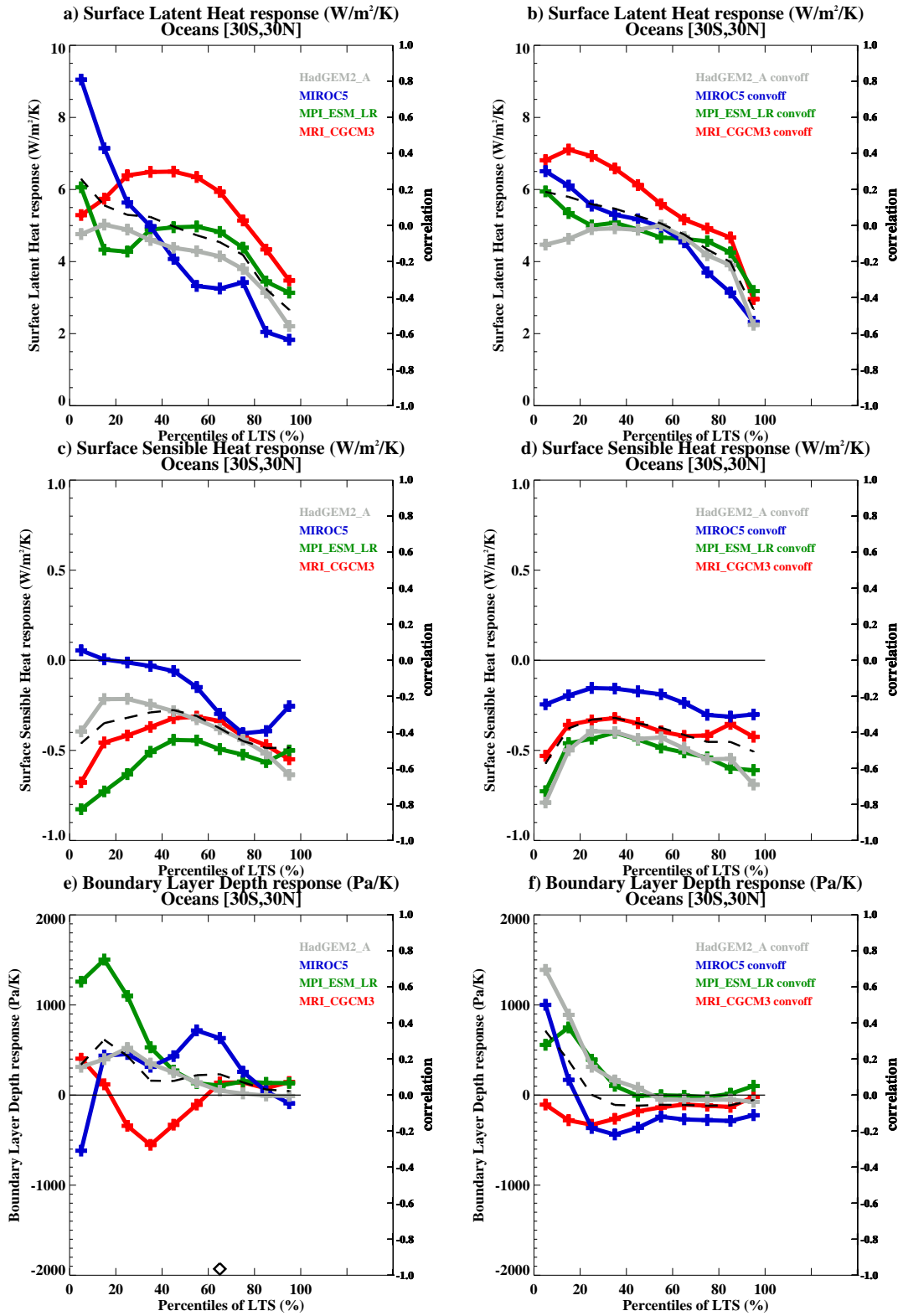


**Figure 20.** As Figure 17 but for surface latent/sensible heat flux and boundary layer depth responses.

